# Bibliography


1. IIJIMA, S. Helical microtubules of graphitic carbon. **Nature**, 354, 7 november 1991. 56 - 58.

2. SAITO, R.; G. DRESSELHAUS; M. S. DRESSELHAUS. **Physical Properties of Carbon Nanotubes**. [S.l.]: [s.n.], 1998. ISBN ISBN 1-86094-093-5.

3. HARRIS, P. J. F. **Carbon Nanotube Science**. [S.l.]: Cambridge University Press, 2009.

4. CAMPOLONGO, M. J. Site about graduate course on Tight Binding calculations applied to mechanical properties of Carbon Nanotubes. **Site from the Materials Process Design & Control Laboratory, Cornell University**, 2009. Disponivel em: <http://mpdc.mae.cornell.edu/Courses/MAE715/Symposium09/MikeCampolongo-Paper.pdf>. Acesso em: August 2012.

5. GULINO, G.; ET. AL. C2H2 as an active carbon source for a large scale synthesis of carbon nanotubes by chemical vapour deposition. **Applied Catalysis A**, n. General 279, 2005. 89-97.

6. CHARLIER, J. C.; ET AL. Structural and electronic properties of pentagon-heptagon pair defects on carbon nanotubes. **Physical Review B**, 53, n. 16, 15 april 1996. 11108 - 11113.

7. JORIO, A.; DRESSELHAUS, M.; DRESSELHAUS, G. (Eds.). **Carbon Nanotubes**. [S.l.]: Springer- Verlag Berlin Heidelberg, v. 111, 2008.

8. KUZMANY, H.; ET. AL. Functionalization of carbon nanotubes. **Synthetic Metals**, n. 141, p. 113 - 122, 2004.

9. AJAYAN, P. M.; IIJIMA, S.; ET. AL. Opening carbon nanotubes with oxygen and implications for filling, n. 362, p. 522 - 525, 19 march 1993.

10. UGARTE, D.; ET. AL. Filling carbon nanotubes. **Applied Physics A**, n. 67, p. 101 - 105, 1998.

11. CARROLL, D. L.; ET. AL. Effects of Nanodomain Formation on the

. Electronic Structure of Doped Carbon Nanotubes. **Physical Review Letters**, v. 81, n. 11, p. 2332 - 2335, september 1998.

12 CERAGIOLI, H. J.; ET. AL. Synthesis and characterization of boron-
. doped carbon nanotubes; (2008) 052029. **Journal of Physics: Conference Series** , v. 100, 2008. ISSN doi:10.1088/1742-6596/100/5/052029.

13 LARRUDE, D.; ET. AL. Multiwalled carbon nanotubes decorated with
. cobalt oxide nanoparticles. **Journal of Nanomaterials**, p. 5 pages, 2012. ISSN doi: 10.1155/2012/695453.

14 CHEN, C. F.; ET. AL. The characterization of boron-doped carbon
. nanotube arrays. **Diamond and Related Materials**, n. 12, p. 1500 - 1504, 2003.

15 AYALA, P.; ET. AL. A one step approach to B-doped single walled
. carbon nanotubes. **Journal of Materials Chemistry**, n. 18, p. 5676–5681, 2008.

16 HSU, W. K.; ET. AL. Metallic behaviour of boron-containing carbon
. nanotubes. **Chemical Physics Letters**, n. 323, p. 572 - 579, 2000.

17 BLASE, X.; ET. AL. Boron-Mediated Growth of Long Helicity-Selected
. Carbon Nanotubes. **PHYSICAL REVIEW LETTERS**, v. 83, n. 24, december 1999.

18 HSU; ET. AL. Boron-doping effects in carbon nanotubes. **Journal of**
. **Materials Chemistry**, n. 10, p. 1425 - 1429, 2000.

19 LARRUDE, D. G.; ET. AL. Characterization of phosphorus-doped
. multiwalled carbon nanotubes. **Journal of Applied Physics**, n. 111, p. 6 pages, 2012. ISSN doi: 10.1063/1.3695452.

20 SAITO, Y.; ET. AL. Carbon nanocapsules and single-layered
. nanotubes produced with platinum group metals (Ru, Rh, Pd, Os, Ir, Pt) by arc discharge. **Journal of Applied Physics**, n. 80, p. 3062 - 3067, 1996. ISSN doi: 10.1063/1.363166.

21 SINGH, C.; WINDLE, A. Production of aligned carbon nanotubes by
. the CVD injection method. **Physica B**, n. 323, p. 339 - 340, 2002.

22 KIM, S. H.; ET. AL. Aerosol formation of Sea-Urchin-like
. nanostructures of carbon nanotubes on bimetallic nanocomposite particles. **Journal of Nanoparticle Research**, n. 13, p. 139 - 146,

2011.

23. SCHNITZLER, M. C.; ZARBIN, A. J. G. The effect of process variables on the characteristics of carbon nanotubes obtained by spray pyrolysis. **Journal Nanoparticle Research**, n. 10, p. 585–597, 2008. ISSN DOI 10.1007/s11051-007-9289-4.

24. ZHOU, W.; ET. AL. Role of Catalysts in the Surface Synthesis of Single-Walled Carbon Nanotubes. **Nano Research**, n. 2, p. 593-598, 2009.

25. SENGUPTA, J.; JACOB, C. The effect of Fe and Ni catalysts on the growth of multiwalled carbon nanotubes using chemical vapor deposition. **Journal of Nanoparticle Research**, n. 12, p. 457 - 465, 2010.

26. IAIA, A.; ET. AL. Oriented growth of suspended single wall carbon nanotube by Hot Filament CVD. **Thin Solid Films**, n. 501, p. 221 - 223, 2006.

27. HAFNER, J.; ET. AL. Catalytic growth of single-wall carbon nanotubes from metal particles. **Chemical Physics Letters**, n. 296, p. 195–202, 1998.

28. KONG, J.; ET. AL. Chemical vapor deposition of methane for single-walled carbon Nanotubes. **Chemical Physics Letters**, n. 292, p. 567–574, 1998.

29. TIBBETTS, G. G. Why are Carbon Filaments Tubular? **Jounral of Crystal Growth**, v. 66, n. 3, p. 632 - 638, 1984.

30. BOLTON, K.; ET. AL. Atomistic Simulations of Catalyzed Carbon Nanotube Growth. **Jounral of Nanoscience and Nanotechnology**, v. 6, n. 5, p. 1211 - 1224, 2006.

31. GAI, P.; ET. AL. Structural systematics in boron-doped single wall carbon nanotubes. **Journal of Materials Chemistry**, n. 14, p. 669 - 675, 2004.

32. MCGUIRE, K.; ET. AL. Synthesis and Raman characterization of boron-doped single-walled carbon nanotubes. **Carbon**, n. 43, p. 219 - 227, 2005.

33 YU, J.; ET. AL. Highly oriented rich boron B–C–N nanotubes by bias-assisted hot filament chemical vapor deposition. **Chemical Physics**

. **Letters**, n. 323, p. 529–533, 2000.

34. AYALA, P.; ET. AL. CVD growth of single-walled B-doped carbon nanotubes. **Physica Status Solidi (B)**, v. 245, n. 10, p. 1935–1938, 2008.

35. MONTEIRO, F. H.; ET. AL. Production and Characterization of Boron-Doped Single Wall Carbon. **The Journal of Physical Chemistry C**, n. 116, p. 3281 - 3285, 2012.

36. MONTEIRO, F. **A study on the production and characterization of boron doped single wall carbon nanotubes (Master Thesis)**. Pontificia Universidade Catolica. Rio de Janeiro, p. 81 pages. 2012.

37. LYU, S. C.; ET. AL. Synthesis of boron-doped double-walled carbon nanotubes by catalytic decomposition of tetrahydrofuran and triisopropyl borate. **Carbon**, n. 49, p. 1532 - 1541, 2011.

38. BRANSDEN, B. H.; JOACHAIN, C. J. **Physics of Atoms and Molecules**. 2. ed. [S.l.]: Prentice Hall, 2003. 1114 pages p. ISBN ISBN 978-0-582-35692-4.

39. DRESSELHAUS, M. S.; ET. AL. Raman spectroscopy on isolated single wall carbon nanotubes. **Carbon**, n. 40, p. 2043 - 2062, 2002.

40. KIM, U. J.; ET. AL. Infrared-Active Vibrational Modes of Single-Walled Carbon Nanotubes; PRL 95, 157402 (2005) PHYSICAL REVIEW LETTERS. **Physical Review Letters**, n. 95, 2005.

41. MOULDER, J. F.; ET. AL. **Handbook of X-ray Photoelectron Spectroscopy**. 1. ed. [S.l.]: Perkin-Elmer Corporation, Physical Electronics Division, 1992. 261 pages p. ISBN ISBN: 0-9627026-2-5.

42. WALLACE, P. R. Band theory of grafite. **Physical Review**, v. 71, n. 9, may 1947.

43. SLONCZEWSKI, J. C.; WEISS, P. R. Band Structure of Graphite. **Physical Review**, v. 109, n. 2, january 1958.

44. SAITO, R.; DRESSELHAUS, G.; DRESSELHAUS, M. S. **Physical Properties of Carbon Nanotubes**. 1. ed. [S.l.]: Imperial College Press, 1998. ISBN ISBN 1-86094-093-5.

45. KATAURA, H.; ET. AL. Optical Properties of Single-Wall Carbon

. Nanotubes. **Synthetic Metals**, n. 103, p. 2555 - 2558, 1999.

46 BACHILO, S. M.; ET. AL. Structure-Assigned Optical Spectra of Single-
. Walled Carbon Nanotubes. **Science**, n. 298, p. 2361 - 2366, 2002.

47 LEFEBVRE, J.; ET. AL. Photoluminescence from an individual single-
. walled carbon nanotube. **Physical Review B**, n. 69, 2004.

48 O'CONNELL, M. J.; ET. AL. Band Gap Fluorescence from Individual
. Single-Walled Carbon Nanotubes. **Science**, n. 297, p. 593 - 596, july 2002.

49 RAO, A. M.; ET. AL. Diameter Selective Raman Scattering from
. Vibrational Modes in Carbon Nanotubes. **Science**, n. 275, p. 187 - 191, 1997. ISSN DOI: 10.1126/science.275.5297.187.

50 JORIO, A.; ET. AL. Characterizing carbon nanotube samples with
. resonance Raman scattering. **New Journal of Physics**, v. 139.1 - 139.17, n. 5, 2003.

51 DRESSELHAUS, M. S.; EKLUND, P. C. Phonons in carbon nanotubes.
. **Advanced in Physics**, v. 49, n. 6, p. 705 - 814, 2000.

52 JORIO, A.; ET. AL. Structural (n,m) Determination of Isolated Single-
. Wall Carbon Nanotubes by Resonant Raman Scattering. **Physical Review Letters**, v. 86, n. 6, p. 1118 - 1121, february 2001.

53 ARAUJO, P. T.; ET. AL. Third and Fourth Optical Transitions in
. Semiconducting Carbon Nanotubes. **Physical Review Letters**, n. 98, february 2007.

54 RAO, A. M.; ET. AL. Raman spectroscopy of pristine and doped single
. wall carbon nanotubes. **Thin Solid Films**, n. 331, p. 141 - 147, 1998.

55 JORIO, A.; ET. AL. G-band resonant Raman study of 62 isolated
. single-wall carbon nanotubes. **Physical Review B**, v. 65, p. 155412-1 - 155412-9, march 2002.

56 FILHO, A. G. S.; ET. AL. Anomalous two-peak G'-band Raman effect
. in one isolated single-wall carbon nanotube. **Physical Review B**, v. 65, p. 085417-1 - 085417-8, 2002.

57 YI, J.-Y.; BERNHOLC, J. Atomic structure and doping of microtubules.
. **Physical Review B**, v. 47, n. 3, p. 1708 - 1711, january 1993.

58. FUENTES, G. G.; ET. AL. Formation and electronic properties of BC3 single-wall nanotubes upon boron substitution of carbon nanotubes. **Physical Review B**, n. 69, p. 245403-1 - 245403-6, 2004.

59. BOROWIAK-PALEN, E.; ET. AL. Synthesis and electronic properties of B-doped single wall carbon nanotubes. **Carbon**, n. 42, p. 1123 - 1126, 2004.

60. DARWENT, B. D. **Bond Dissociation Energies in Simple Molecules**. National Standard Reference Data System - National Bureau of Standards. Washignton D.C., p. 1 - 48. 1970.

61. SUZUKI, S.; HIBINO, H. Characterization of doped single-wall carbon nanotubes by Raman spectroscopy. **Carbon**, n. 49, p. 2264 - 2272, 2011.

62. AYALA, P.; ET. AL. Evidence for substitutional boron doped single-walled carbon nanotubes. **Applied Physics**, Letters, n. 96, p. 3 pages, 2010. ISSN doi:10.1063/1.3427432.

63. REDLICH, P.; ET. AL. B-C-N nanotubes and boron doping of carbon nanotubes. **Chemical Physics Letters**, v. 260, p. 465 - 470, September 1996.

64. XU, E.; ET. AL. Doped carbon nanotube array with a gradient of nitrogen concentration. **Carbon**, n. 48, p. 3097 - 3102, 2010.

65. GRIMM, D.; ET. AL. Catalytic decomposition of n-heptane for the growth of high quality single wall carbon nanotubes. **Chemical Physics Letters**, n. 428, p. 416 - 420, 2006.

66. CHRISTOPHER, P. M.; SHILMAN, A. Vapor Pressures of Trialkyl Borates. **Journal of Chemical & Engineering Data**, v. 12, n. 3, p. 333 - 335, july 1967.

67. JACQUES, S.; ET. AL. LPCVD and characterization of boron-containing pyrocarbon materials. **Carbon**, v. 34, n. 9, p. 1135 - 1143, 1996.

68. CERMIGNANI, W.; ET. AL. Synthesis and characterization of boron-doped carbons. **Carbon**, v. 33, n. 4, p. 367 - 374, 1995.

69. JACOBSOHN, L. G.; ET. AL. X-Ray photoelectron spectroscopy investigation of boron carbide films deposited by sputtering. **Surface**

**Science**, n. 572, p. 418 - 424, 2004.

70. BYSTRZEJEWSKI, M.; ET, AL. Boron doped carbon nanotubes via ceramic catalysts. **Physica Status Solidi Rapid Research Letters**, v. 3, n. 6, p. 193 - 195, 2009.

71. JIAN-GANG, Q.; ET. AL. Formation mechanism of pulse current anodized film on AZ91D Mg alloy. **Transactions of Nonferrous Metals Society of China**, n. 18, p. 19 - 23, 2008.

72. HASHIM, D. P.; ET. AL. Covalently bonded three-dimensional carbon nanotube solids via boron induced nanojunctions. **Scientific Reports**, v. 2, n. 363, p. 1 - 8, april 2012. ISSN doi:10.1038/srep00363.

73. WIRTZ, L.; RUBIO, A. Band structure of boron doped carbon nanotubes. **AIP Conference Proceedings**, v. 685, n. 402, p. 4 pages, 2003. ISSN DOI: 10.1063/1.1628059.

74. QINGBO, W.; AL., E. First-principles calculations on the structure and electronic properties of boron doping zigzag single-walled carbon nanotubes. **Science in China Series E: Technological Sciences**, v. 52, n. 5, p. 1219 - 1224, may 2009.

75. TIAN-BAO, L.; ET. AL. Preparation and Characteriztic of one-dimensional magnesium borate nanomaterials. **Journal of Inorganic Materials**, v. 25, n. 9, p. 947 - 951, september 2010.

76. MACIEL, I. O.; ET. AL. Electron and phonon renormalization near charged defects in carbon nanotubes. **Nature Materials**, v. 7, p. 878 - 883, november 2008.

77. BRIGGS, D.; BEAMSON, G. XPS studies of the oxygen 1s and 2s levels in a wide range of functional polymers. **Analytical Chemistry**, n. 65, p. 1517 - 1523, 1993.

# 6 Appendix

In this chapter characteristic Raman and XPS measurements will be displayed for each Experiment Run. This way, will be able to further understand the remarks and the numbers along the “Results” chapter.

In relation to XPS, the survey, $C1s$, and $B1s$ spectra are displayed; and the tables present in each graph correspond to the values found in the “Results” chapter.

In relation to Raman, the $G$ band spectra, as well as the survey spectra are displayed. The RBM spectra are absent from this Appendix because they are already displayed in Figure 32. The $G$ band spectra presents the measurement as a black line, the fitted peaks as green lines, and their sum (adjusted curve) as a red line; no quantitative values are displayed, though, because the displayed spectra are single measurements, while the information in the “Results” chapter consider all measurements undertaken for each Experiment Run. The Raman spectra serve to give a qualitative idea about the samples and the quality of the fits.

**Experiment Run 1:**

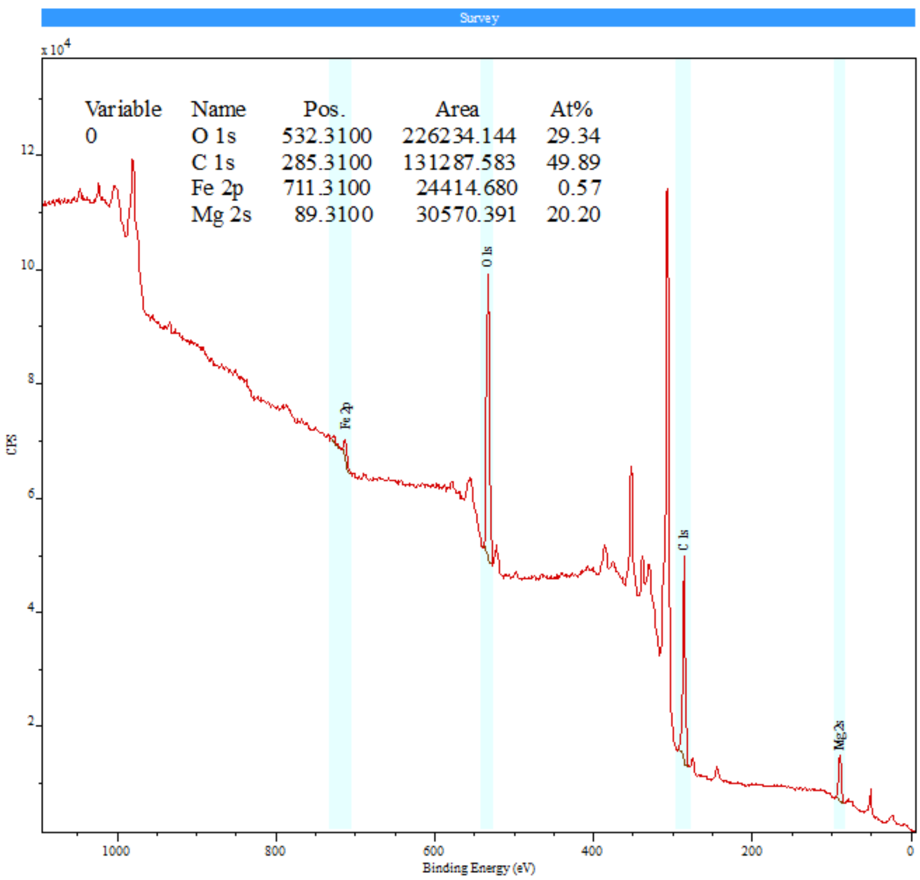

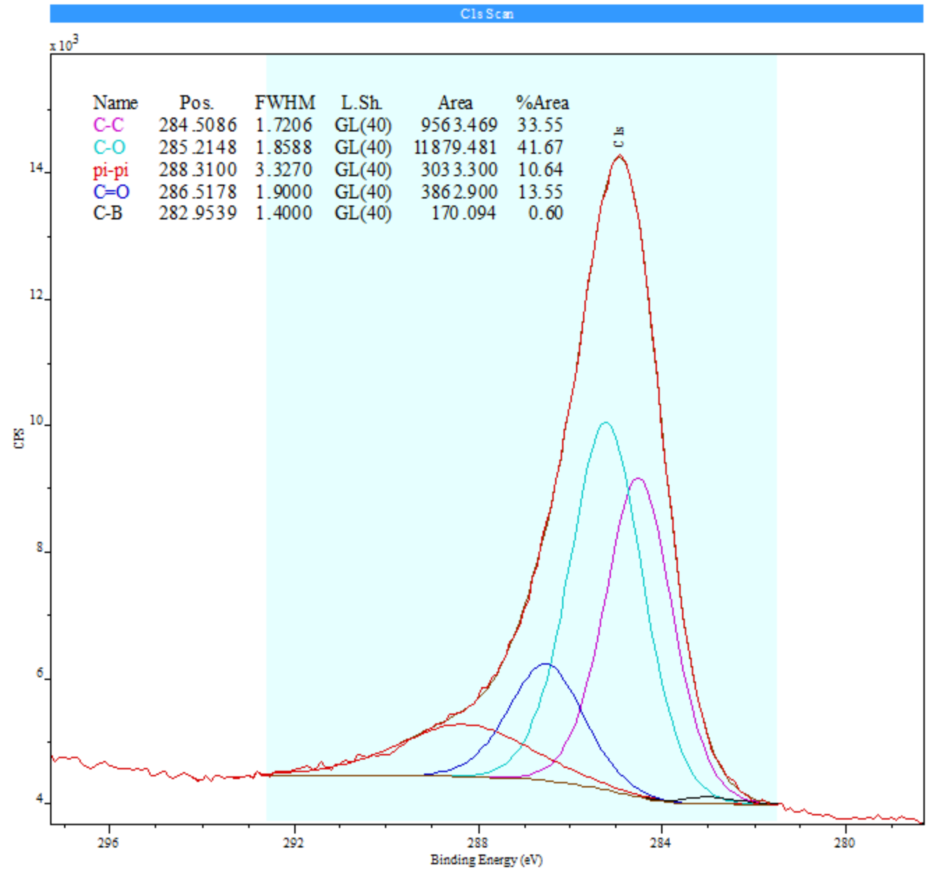
C1s Scan
x 10^3
Name Pos. FWHM L.Sh. Area %Area
C-C 284.5086 1.7206 GL(40) 9563.469 33.55
C-O 285.2148 1.8588 GL(40) 11879.481 41.67
pi-pi 288.3100 3.3270 GL(40) 3033.300 10.64
C=O 286.5178 1.9000 GL(40) 3862.900 13.55
C-B 282.9539 1.4000 GL(40) 170.094 0.60
C 1s
CPS
14
12
10
8
6
4
296
292
288
284
280
Binding Energy (eV)

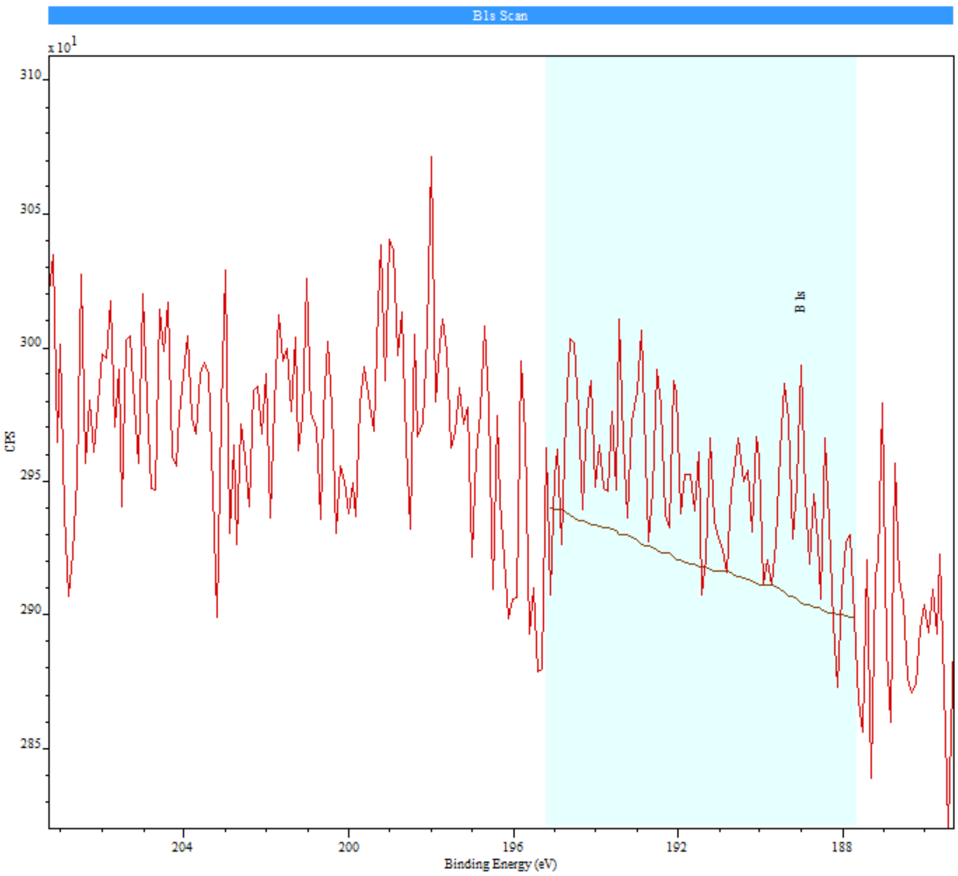
B1s Scan
x 10^1
B 1s
CPS
310
305
300
295
290
285
204
200
196
192
188
Binding Energy (eV)

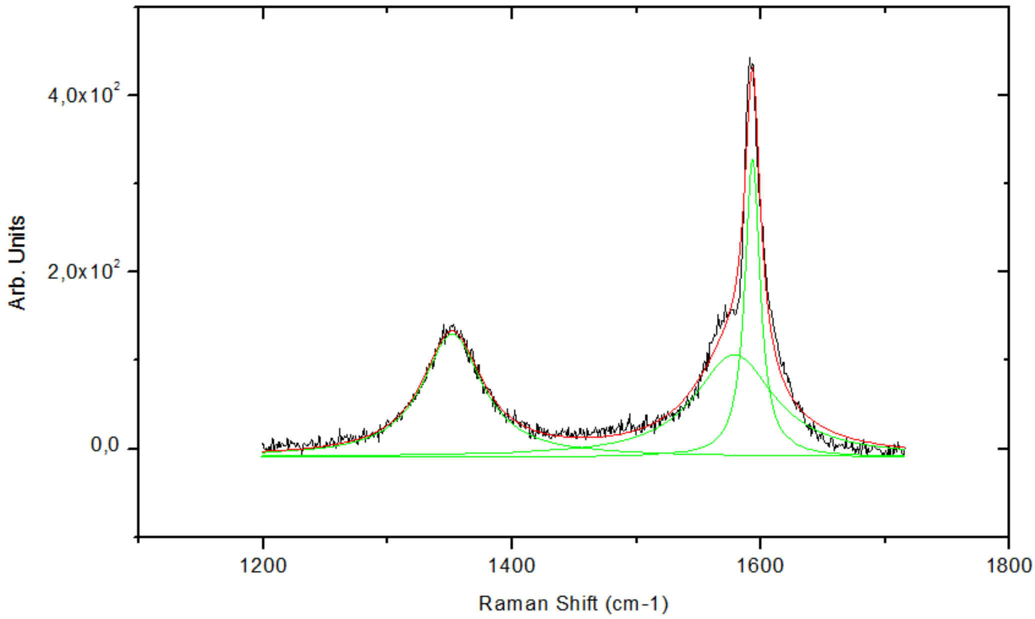
4,0x10^2
2,0x10^2
0,0
Arb. Units
1200
1400
1600
1800
Raman Shift (cm-1)

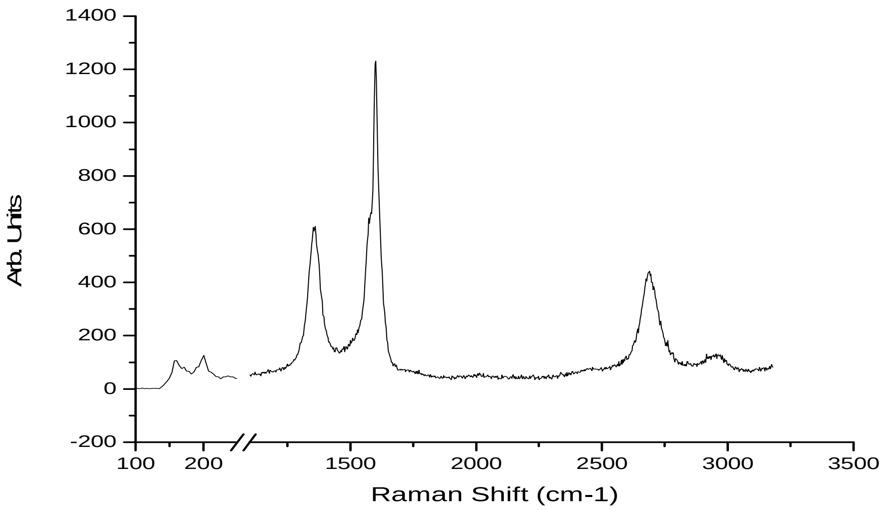
1400
1200
1000
800
600
400
200
0
-200
Arb. Units
100
200
1500
2000
2500
3000
3500
Raman Shift (cm-1)

**Experiment Run 2:**

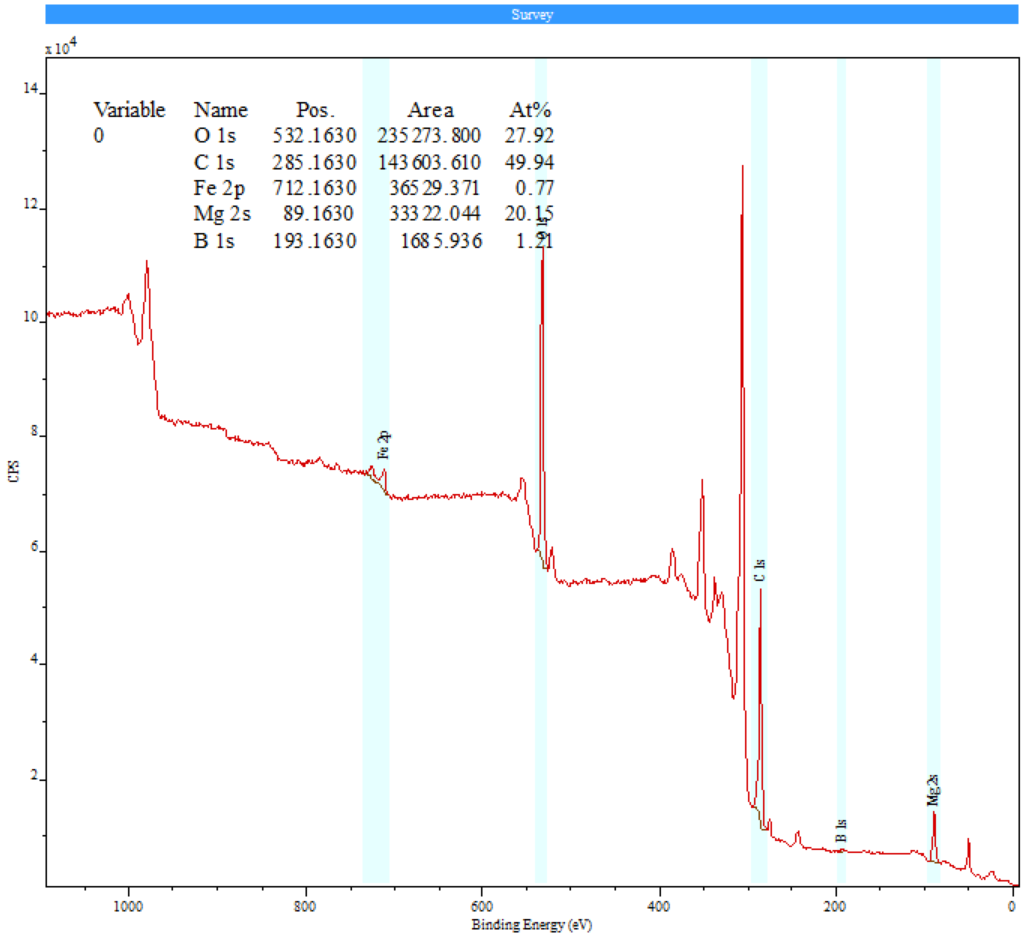

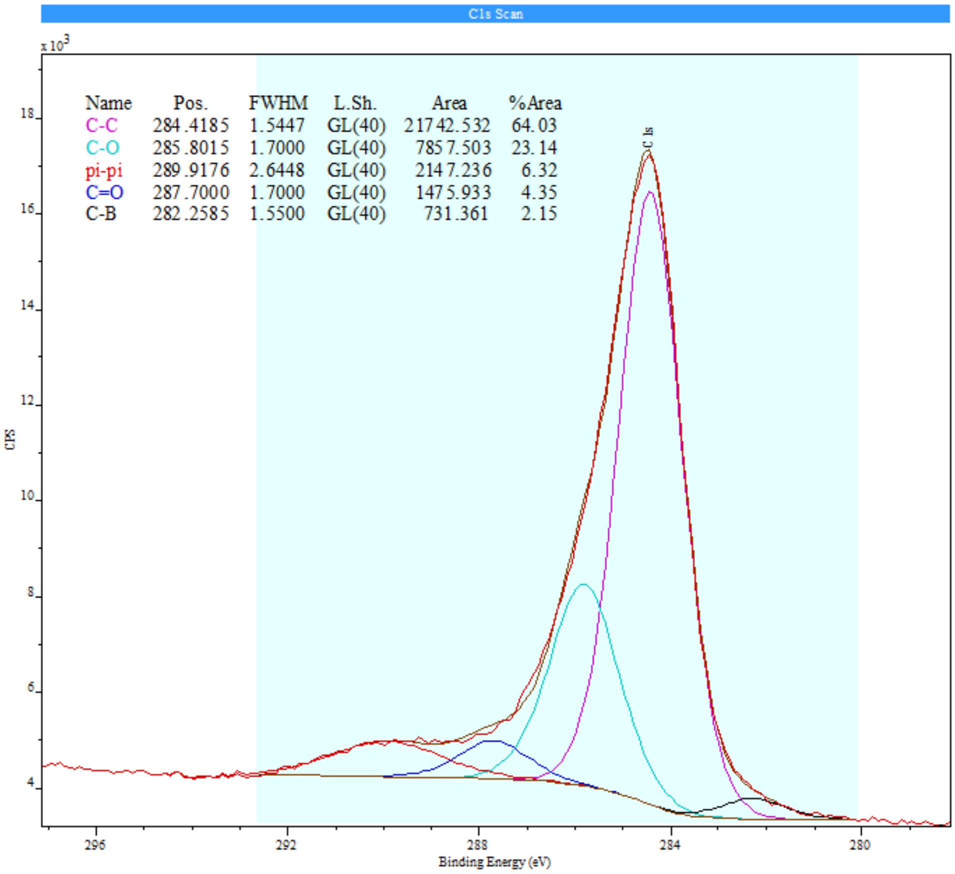
C1s Scan
x 10^3
Name Pos. FWHM L.Sh. Area %Area
C-C 284.4185 1.5447 GL(40) 21742.532 64.03
C-O 285.8015 1.7000 GL(40) 7857.503 23.14
pi-pi 289.9176 2.6448 GL(40) 2147.236 6.32
C=O 287.7000 1.7000 GL(40) 1475.933 4.35
C-B 282.2585 1.5500 GL(40) 731.361 2.15
C 1s
CPS
Binding Energy (eV)

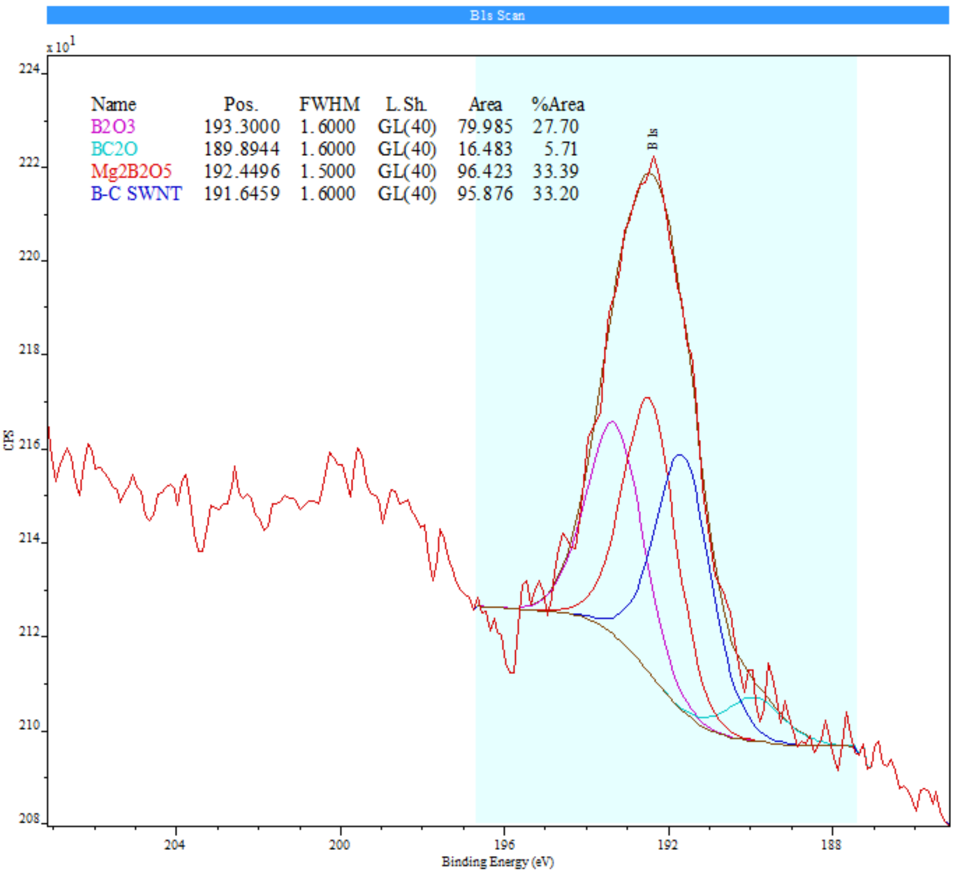
B1s Scan
x 10^1
Name Pos. FWHM L.Sh. Area %Area
B2O3 193.3000 1.6000 GL(40) 79.985 27.70
BC2O 189.8944 1.6000 GL(40) 16.483 5.71
Mg2B2O5 192.4496 1.5000 GL(40) 96.423 33.39
B-C SWNT 191.6459 1.6000 GL(40) 95.876 33.20
B 1s
CPS
Binding Energy (eV)

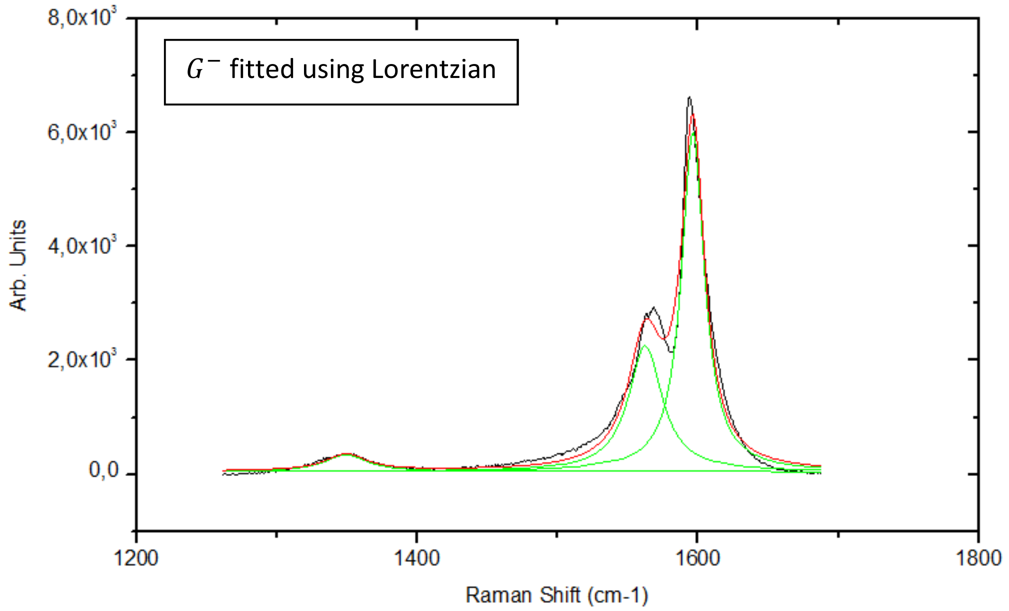

$G^-$ fitted using Lorentzian
8,0x10³
6,0x10³
4,0x10³
2,0x10³
0,0
Arb. Units
1200
1400
1600
1800
Raman Shift (cm-1)


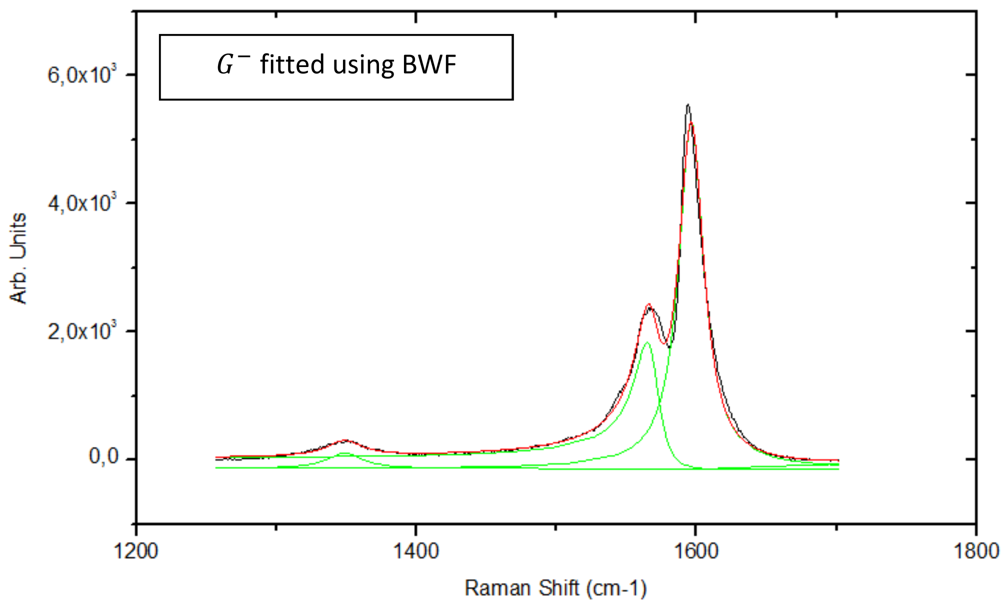

$G^-$ fitted using BWF
6,0x10³
4,0x10³
2,0x10³
0,0
Arb. Units
1200
1400
1600
1800
Raman Shift (cm-1)

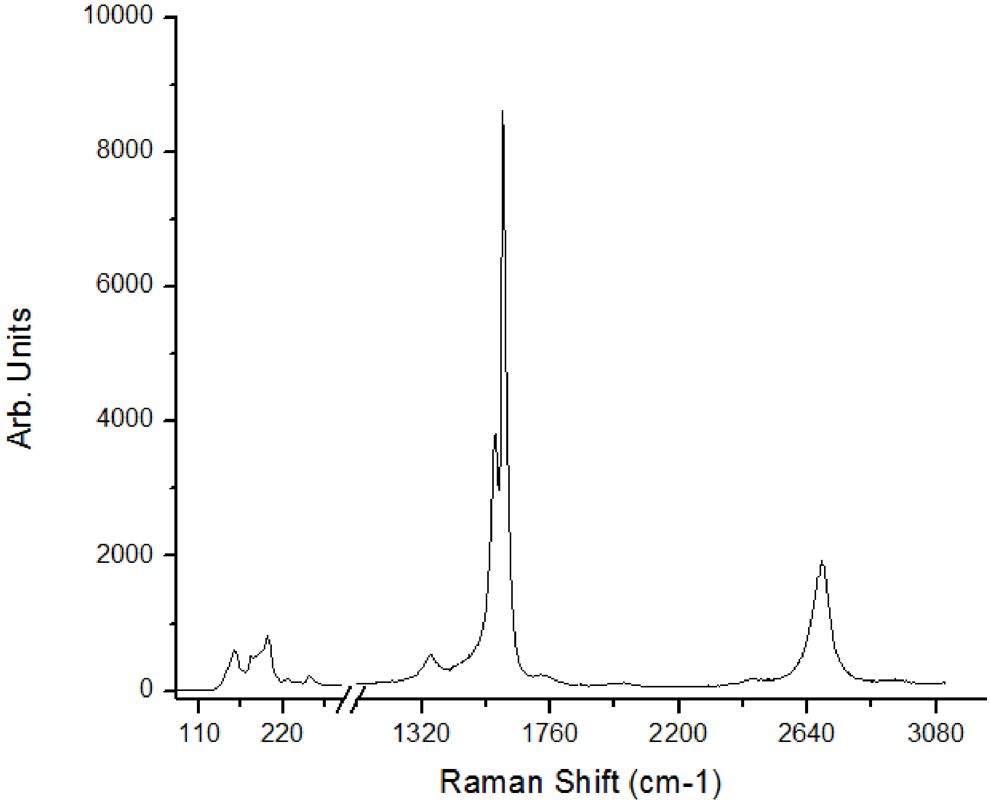


**Experiment Run 3:**

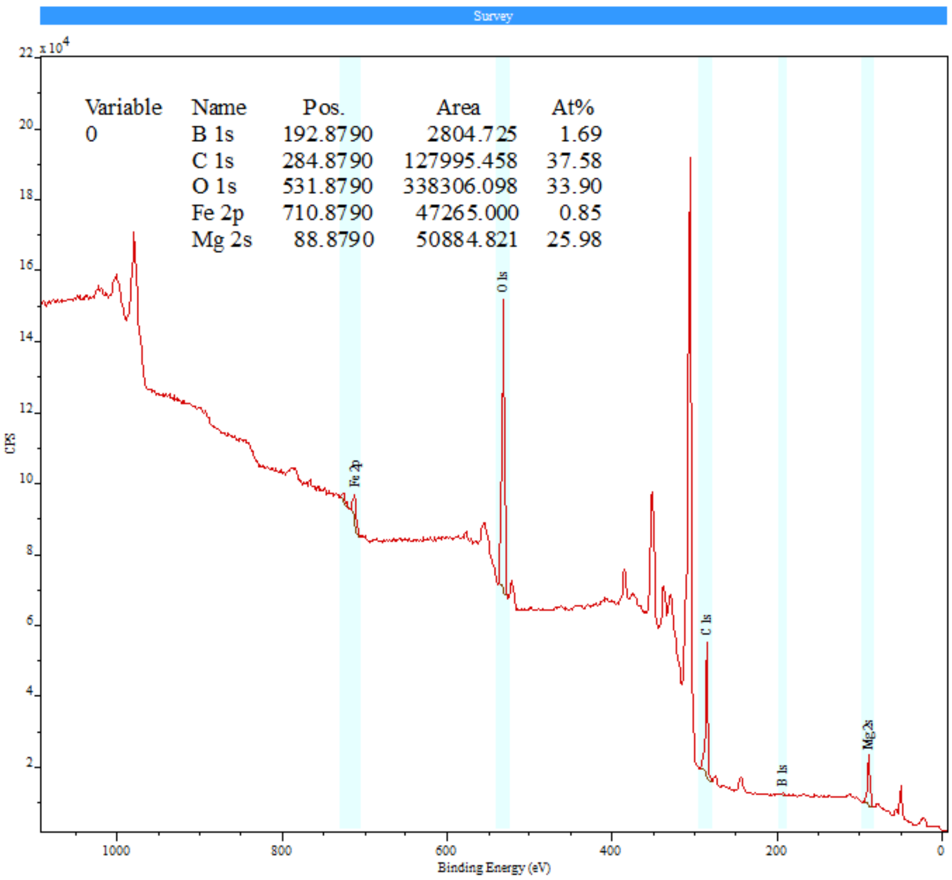

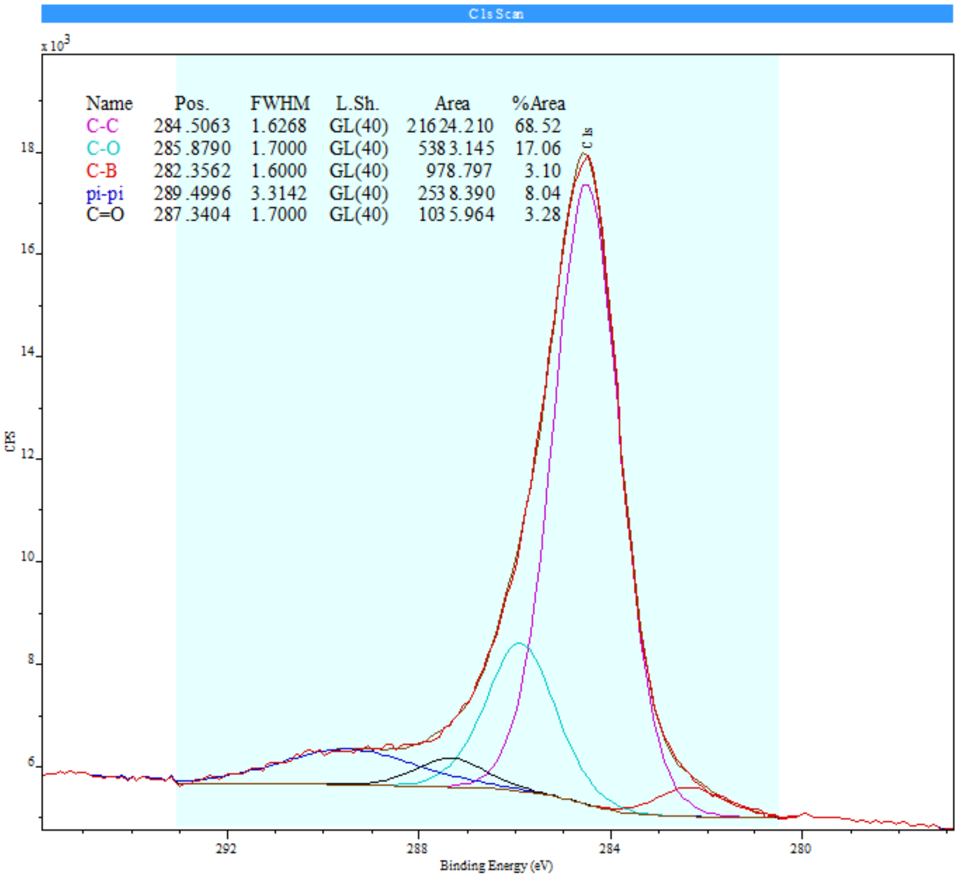
C1s Scan
x 10^3
Name Pos. FWHM L.Sh. Area %Area
C-C 284.5063 1.6268 GL(40) 21624.210 68.52
C-O 285.8790 1.7000 GL(40) 5383.145 17.06
C-B 282.3562 1.6000 GL(40) 978.797 3.10
pi-pi 289.4996 3.3142 GL(40) 2538.390 8.04
C=O 287.3404 1.7000 GL(40) 1035.964 3.28
C 1s
CPS
Binding Energy (eV)

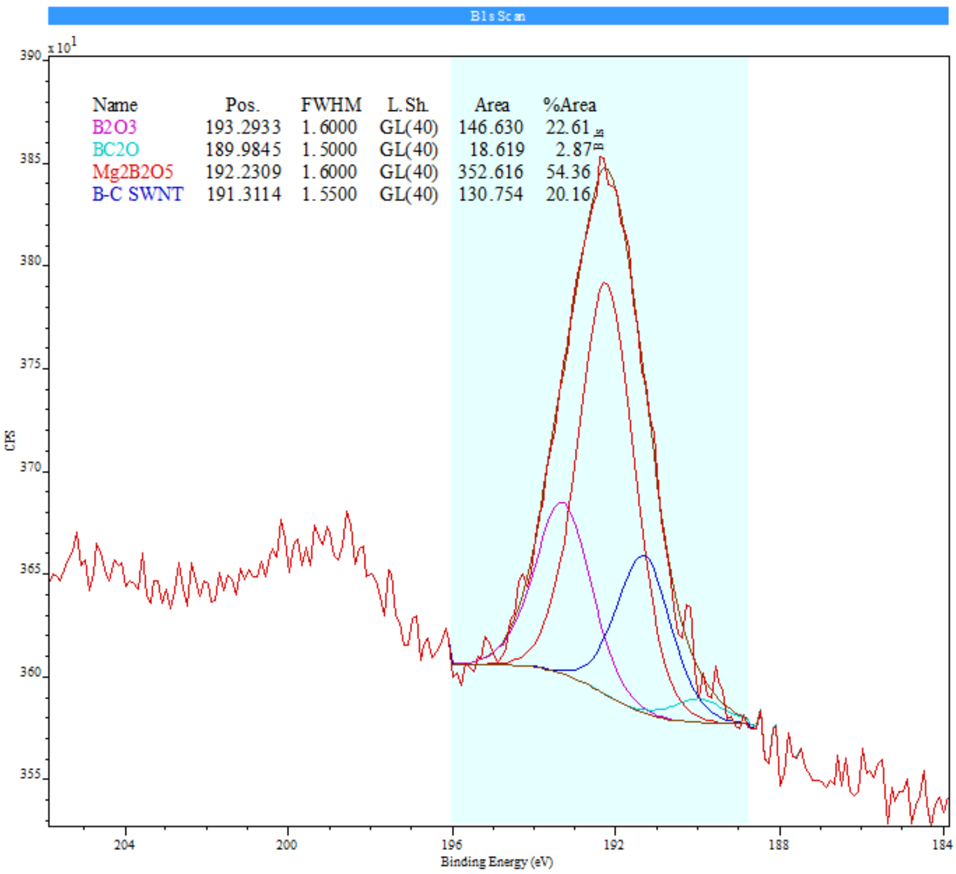
B1s Scan
x 10^1
Name Pos. FWHM L.Sh. Area %Area
B2O3 193.2933 1.6000 GL(40) 146.630 22.61
BC2O 189.9845 1.5000 GL(40) 18.619 2.87
Mg2B2O5 192.2309 1.6000 GL(40) 352.616 54.36
B-C SWNT 191.3114 1.5500 GL(40) 130.754 20.16
B 1s
CPS
Binding Energy (eV)

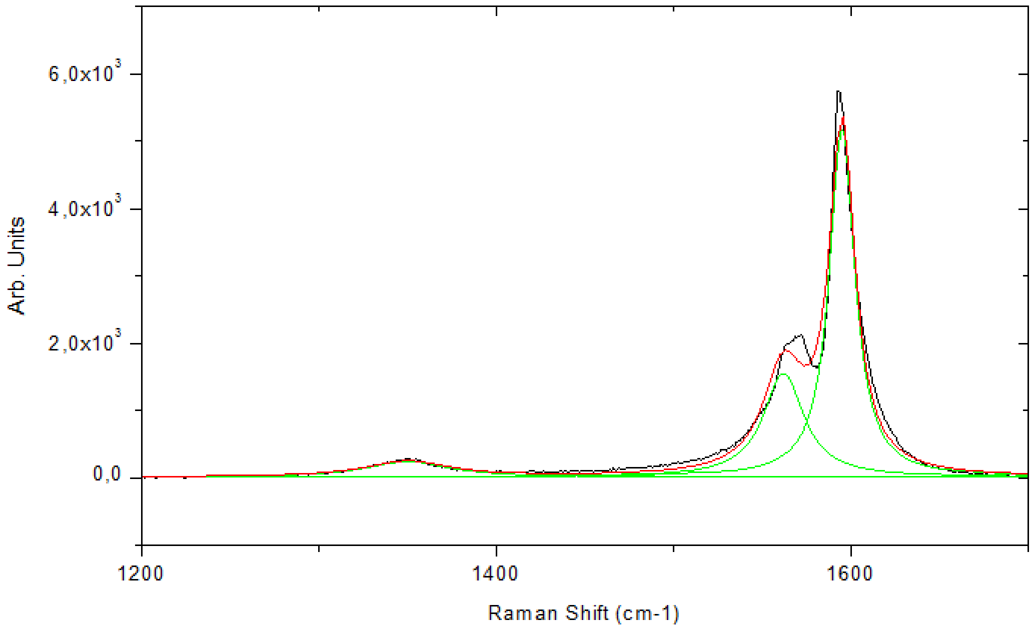
6,0x10^3
4,0x10^3
2,0x10^3
0,0
Arb. Units
1200
1400
1600
Raman Shift (cm-1)

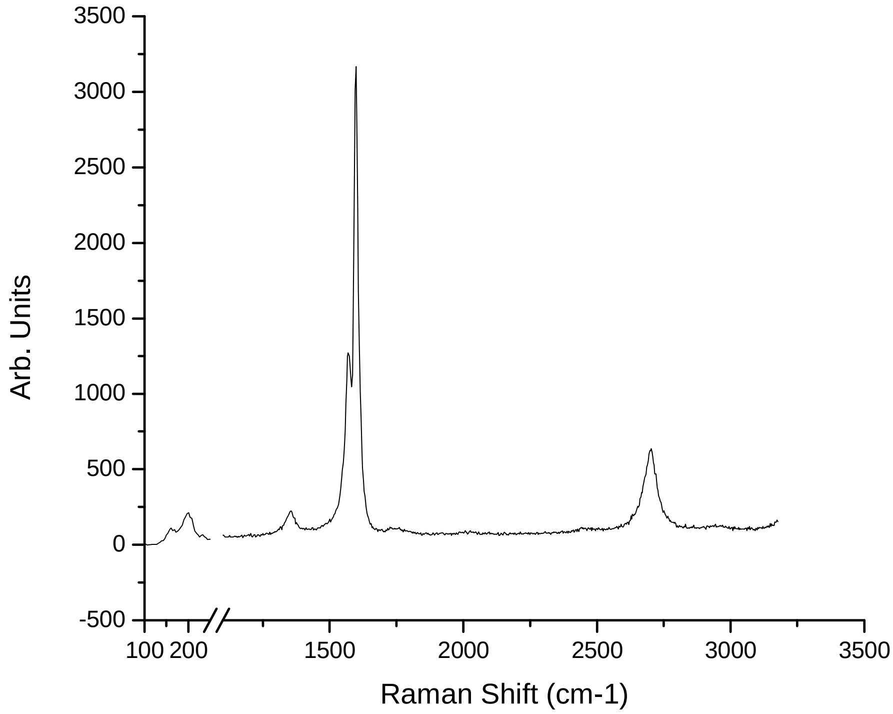
3500
3000
2500
2000
1500
1000
500
0
-500
Arb. Units
100 200
1500
2000
2500
3000
3500
Raman Shift (cm-1)

**Experiment Run 4:**

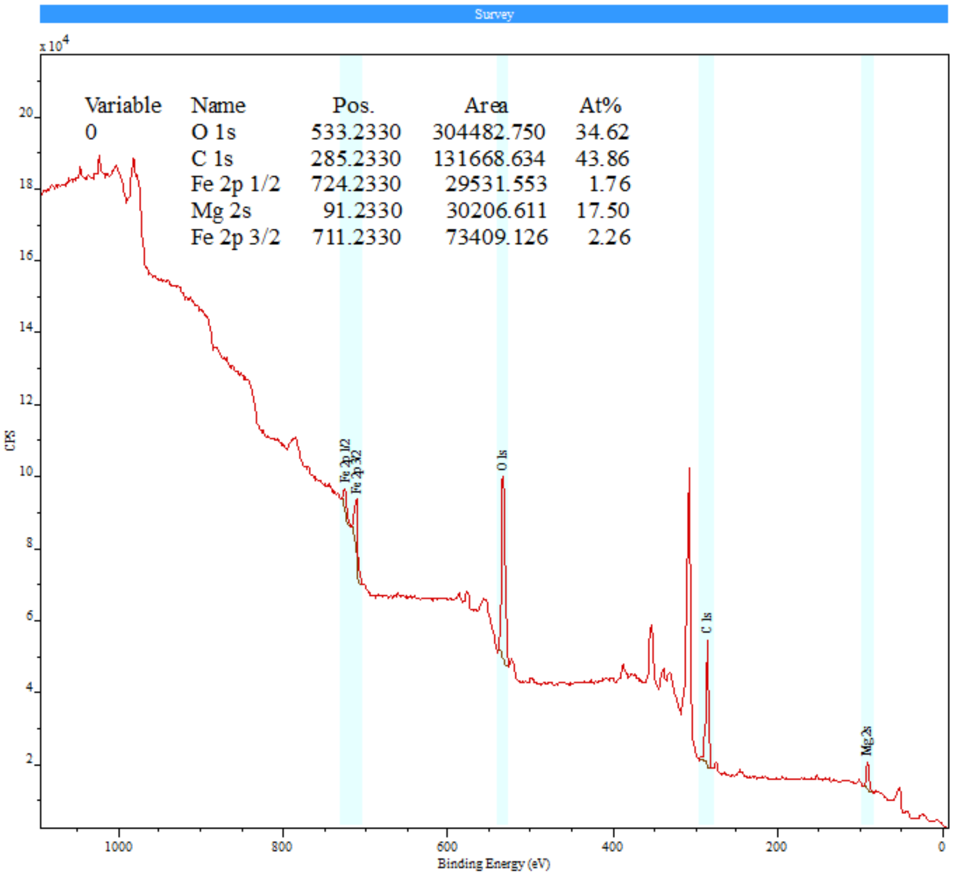

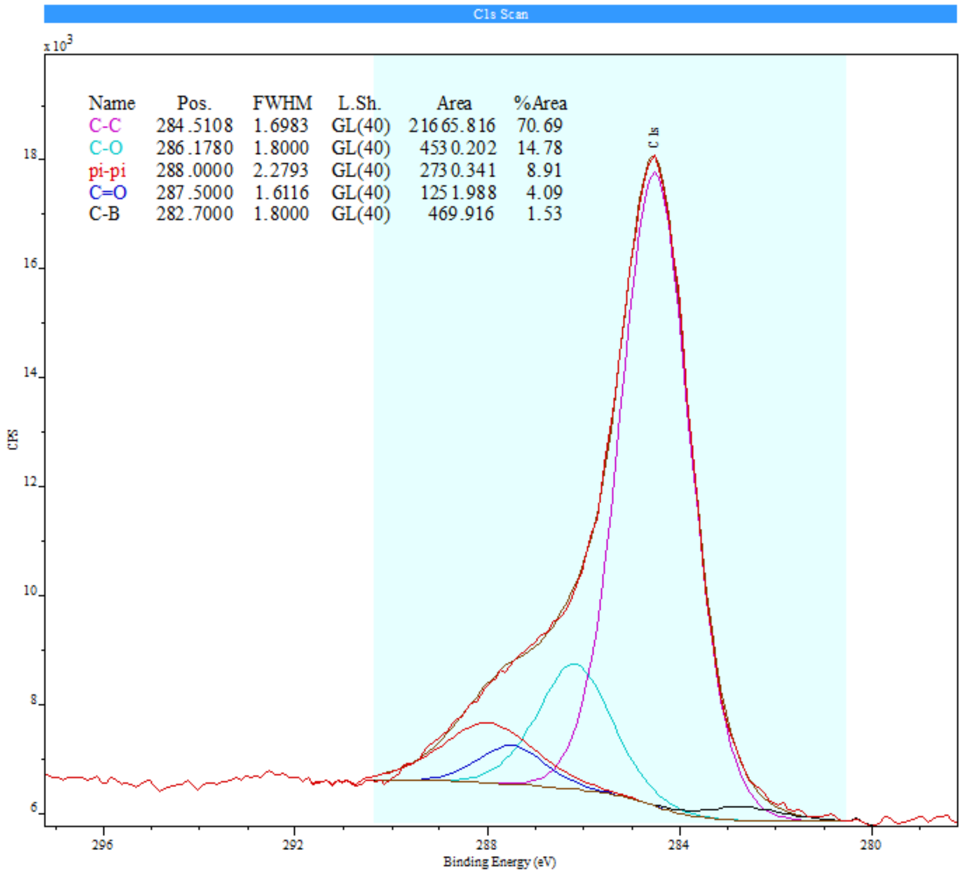
C1s Scan
x 10^3
Name Pos. FWHM L.Sh. Area %Area
C-C 284.5108 1.6983 GL(40) 21665.816 70.69
C-O 286.1780 1.8000 GL(40) 4530.202 14.78
pi-pi 288.0000 2.2793 GL(40) 2730.341 8.91
C=O 287.5000 1.6116 GL(40) 1251.988 4.09
C-B 282.7000 1.8000 GL(40) 469.916 1.53
C 1s
CPS
Binding Energy (eV)

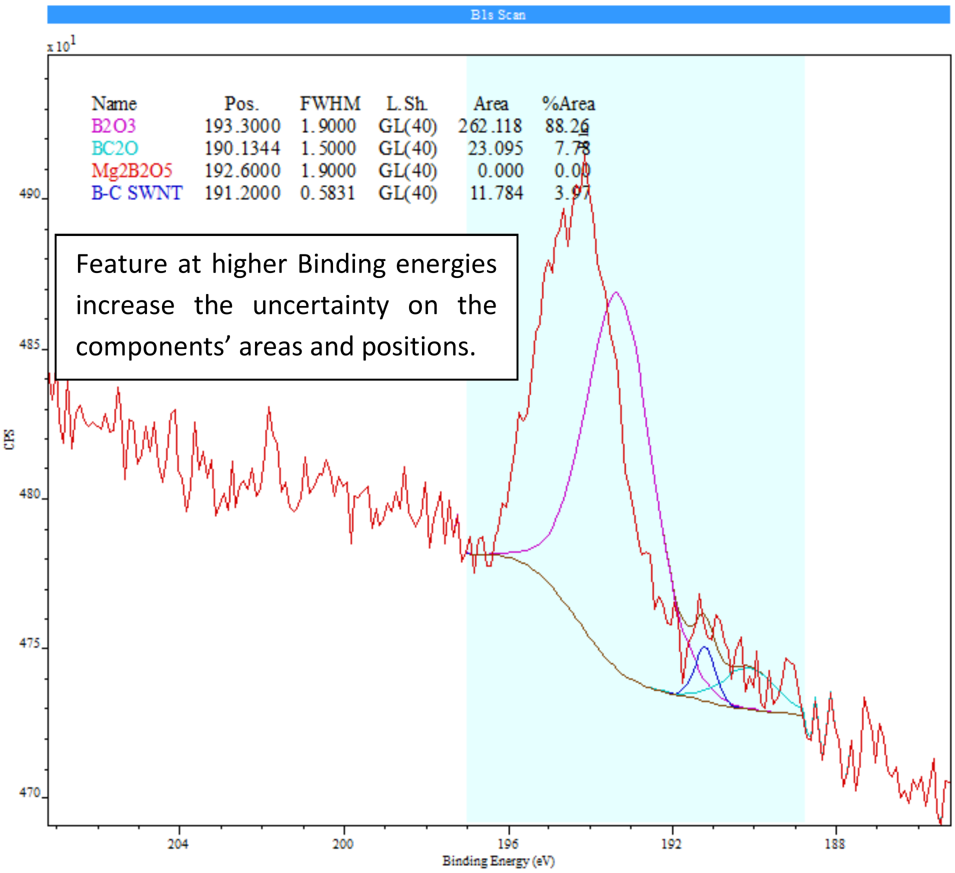
B1s Scan
x 10^1
Name Pos. FWHM L.Sh. Area %Area
B2O3 193.3000 1.9000 GL(40) 262.118 88.26
BC2O 190.1344 1.5000 GL(40) 23.095 7.78
Mg2B2O5 192.6000 1.9000 GL(40) 0.000 0.00
B-C SWNT 191.2000 0.5831 GL(40) 11.784 3.97
Feature at higher Binding energies increase the uncertainty on the components' areas and positions.
CPS
Binding Energy (eV)

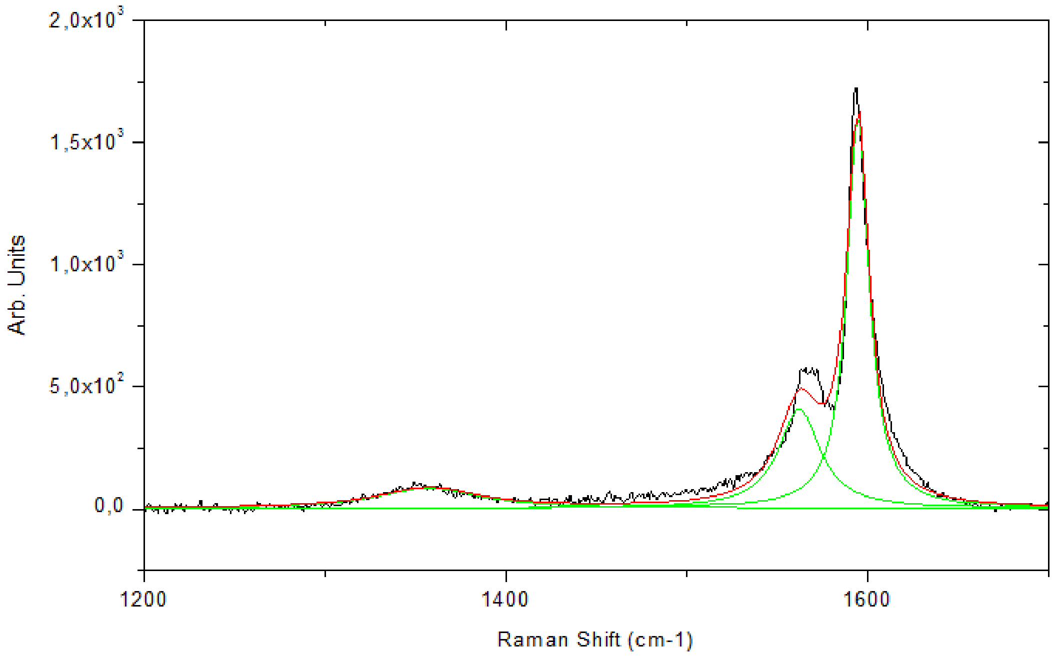
2,0x10^3
1,5x10^3
1,0x10^3
5,0x10^2
0,0
Arb. Units
1200
1400
1600
Raman Shift (cm-1)



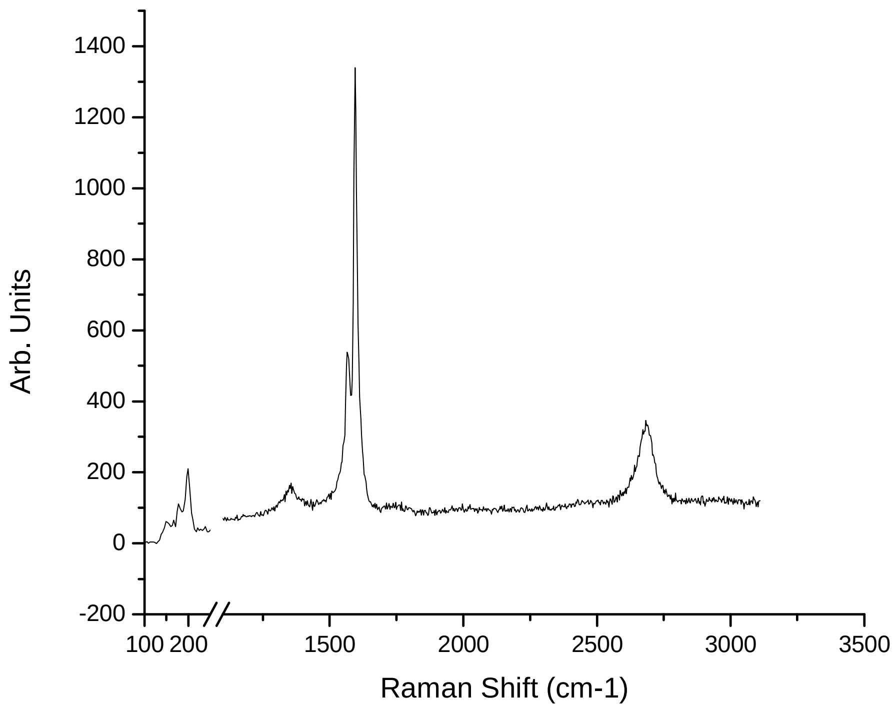
1400
1200
1000
800
600
400
200
0
-200
Arb. Units
100 200
1500
2000
2500
3000
3500
Raman Shift (cm-1)

**Experiment Run 5:**

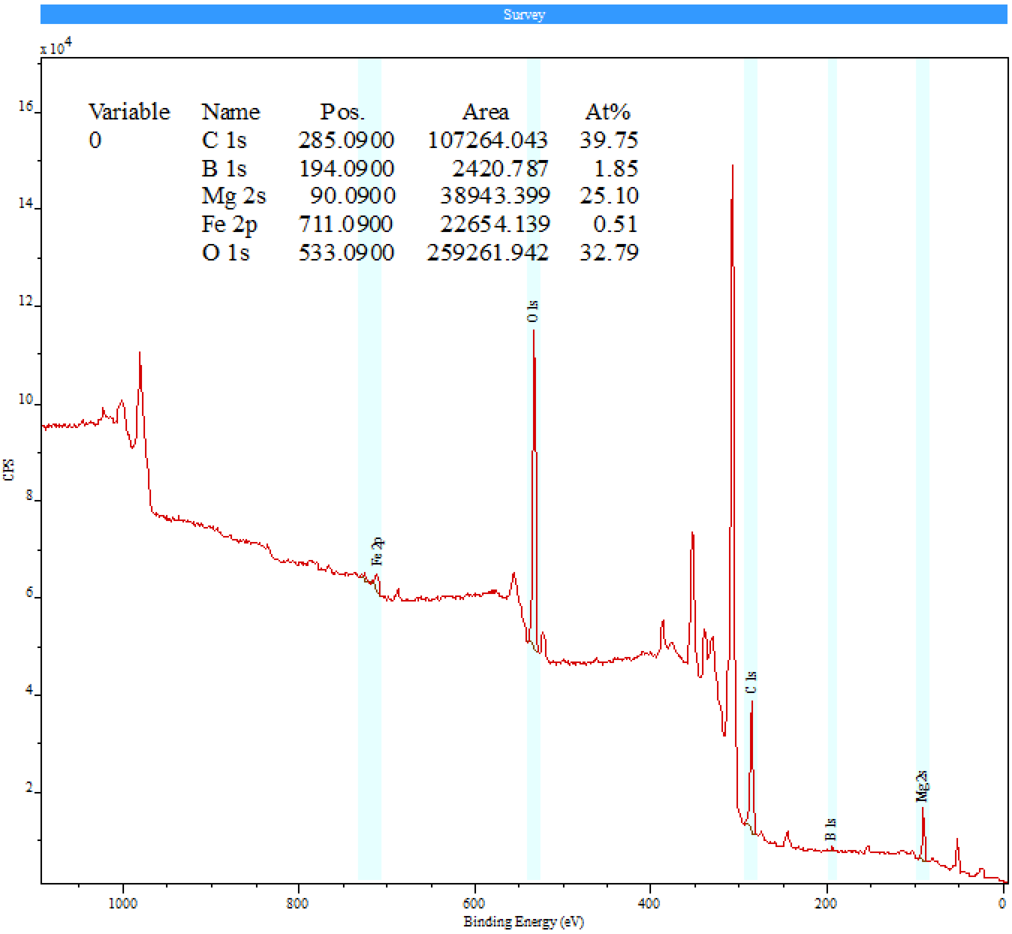

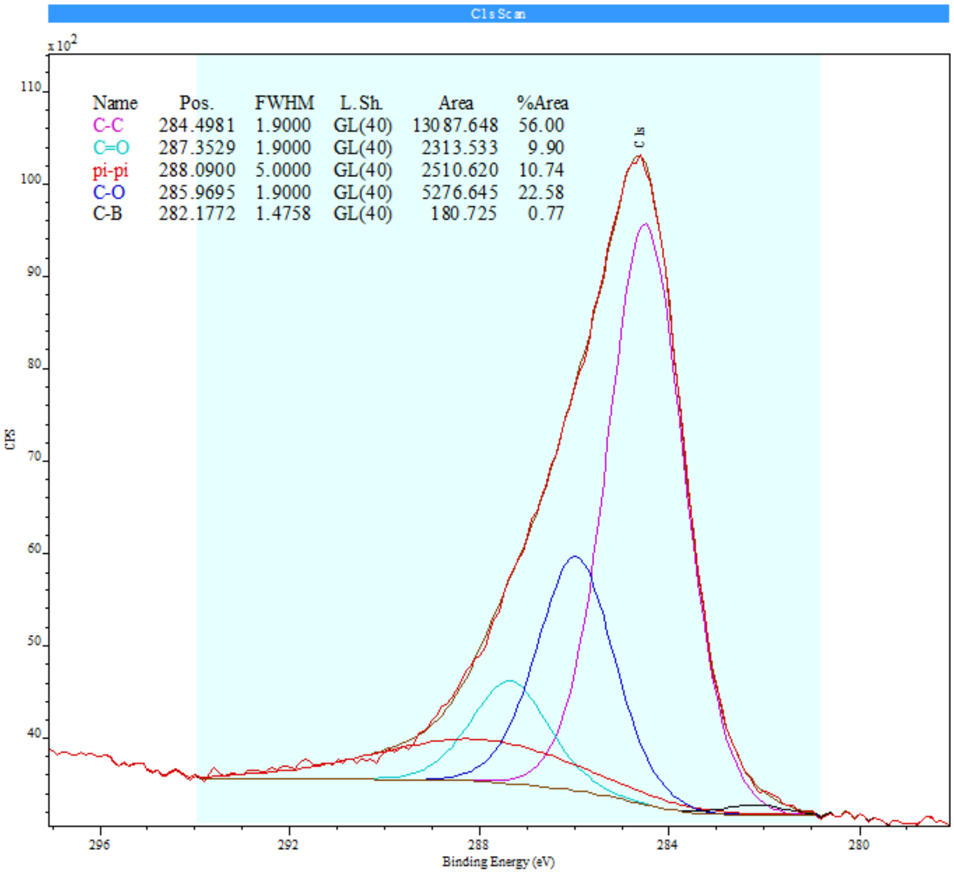
C1s Scan
x 10^2
Name Pos. FWHM L.Sh. Area %Area
C-C 284.4981 1.9000 GL(40) 13087.648 56.00
C=O 287.3529 1.9000 GL(40) 2313.533 9.90
pi-pi 288.0900 5.0000 GL(40) 2510.620 10.74
C-O 285.9695 1.9000 GL(40) 5276.645 22.58
C-B 282.1772 1.4758 GL(40) 180.725 0.77
C 1s
CPS
Binding Energy (eV)

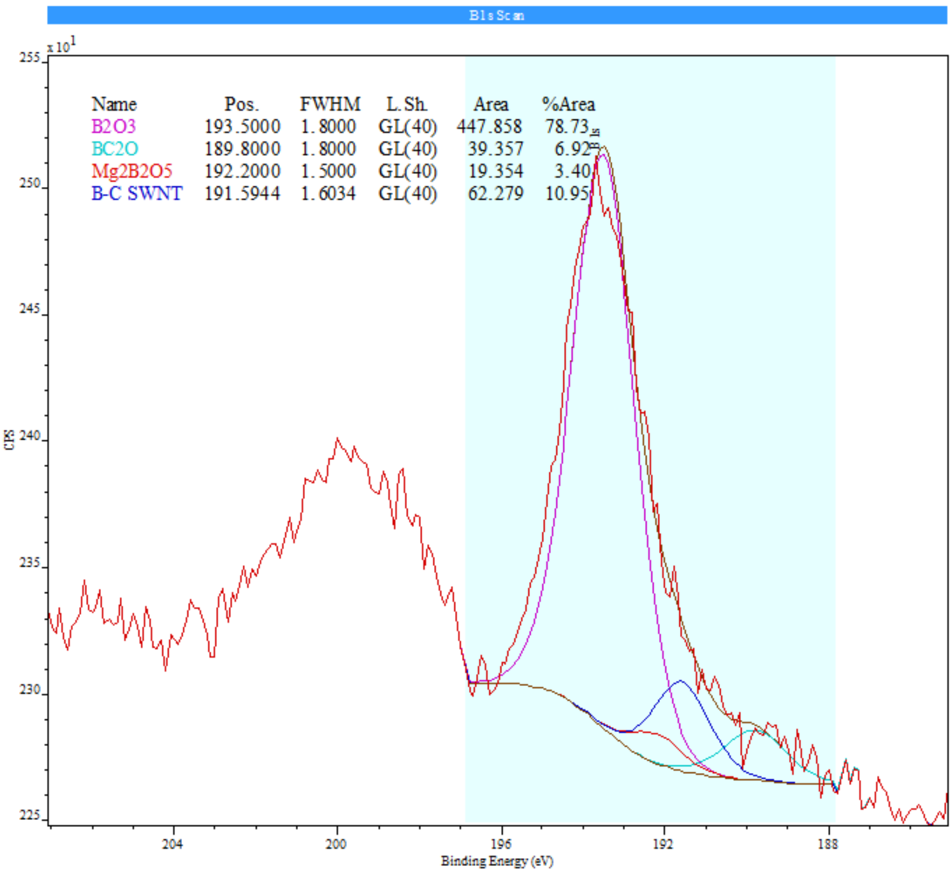
B1s Scan
x 10^1
Name Pos. FWHM L.Sh. Area %Area
B2O3 193.5000 1.8000 GL(40) 447.858 78.73
BC2O 189.8000 1.8000 GL(40) 39.357 6.92
Mg2B2O5 192.2000 1.5000 GL(40) 19.354 3.40
B-C SWNT 191.5944 1.6034 GL(40) 62.279 10.95
CPS
Binding Energy (eV)

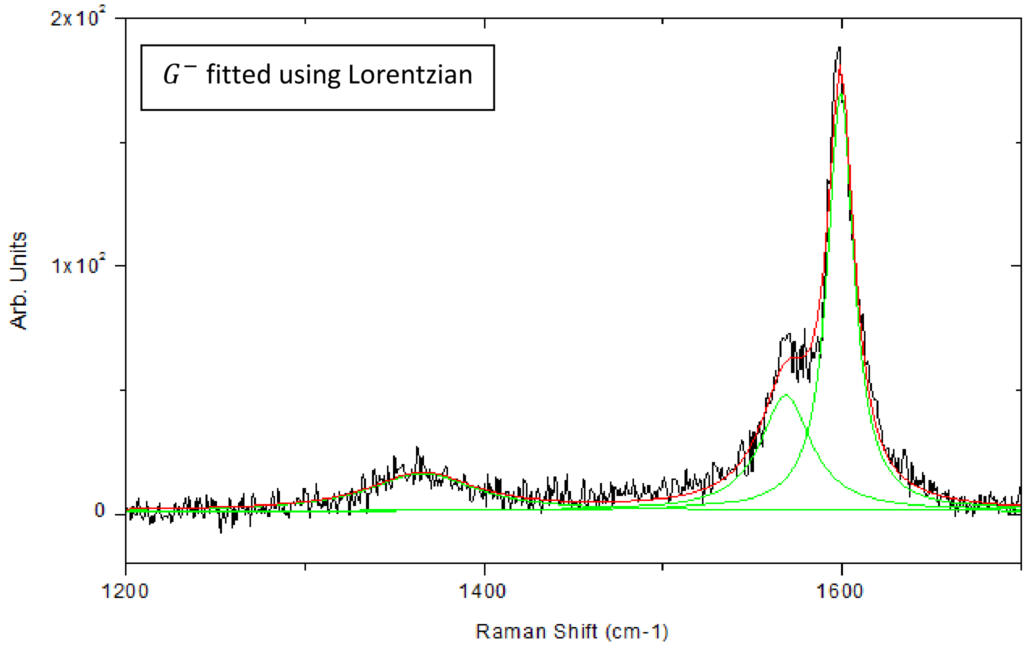
$G^-$ fitted using Lorentzian
2x10²
1x10²
0
Arb. Units
1200
1400
1600
Raman Shift (cm-1)

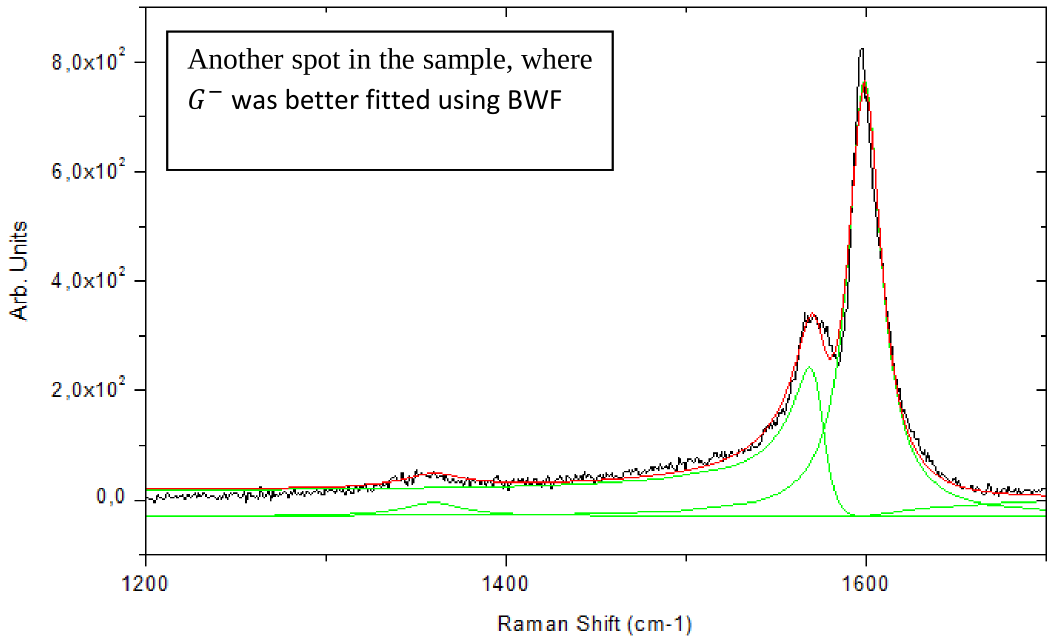
Another spot in the sample, where
$G^-$ was better fitted using BWF
8,0x10²
6,0x10²
4,0x10²
2,0x10²
0,0
Arb. Units
1200
1400
1600
Raman Shift (cm-1)

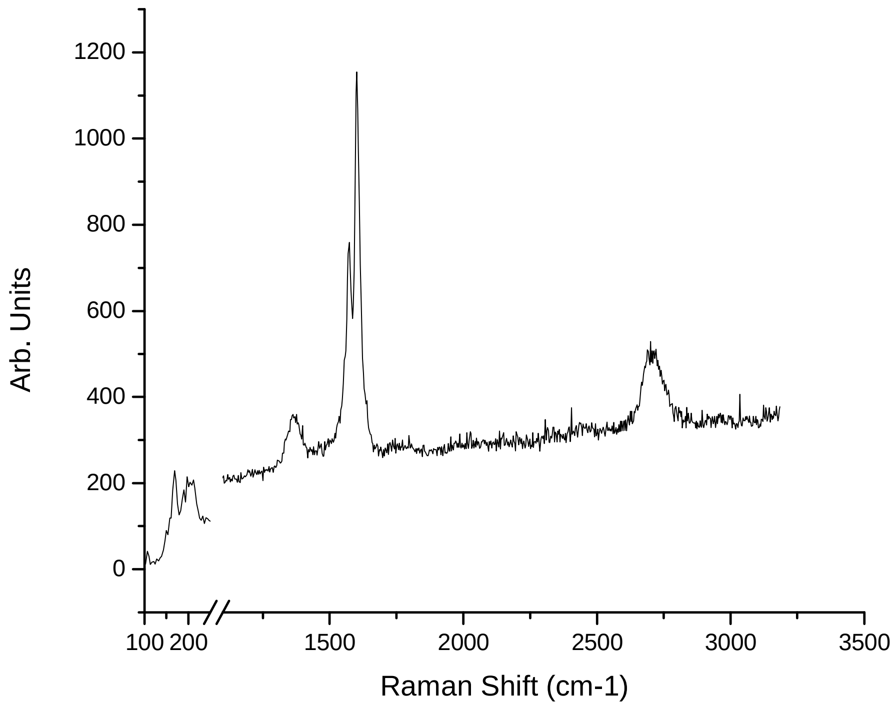


**Experiment Run 6:**

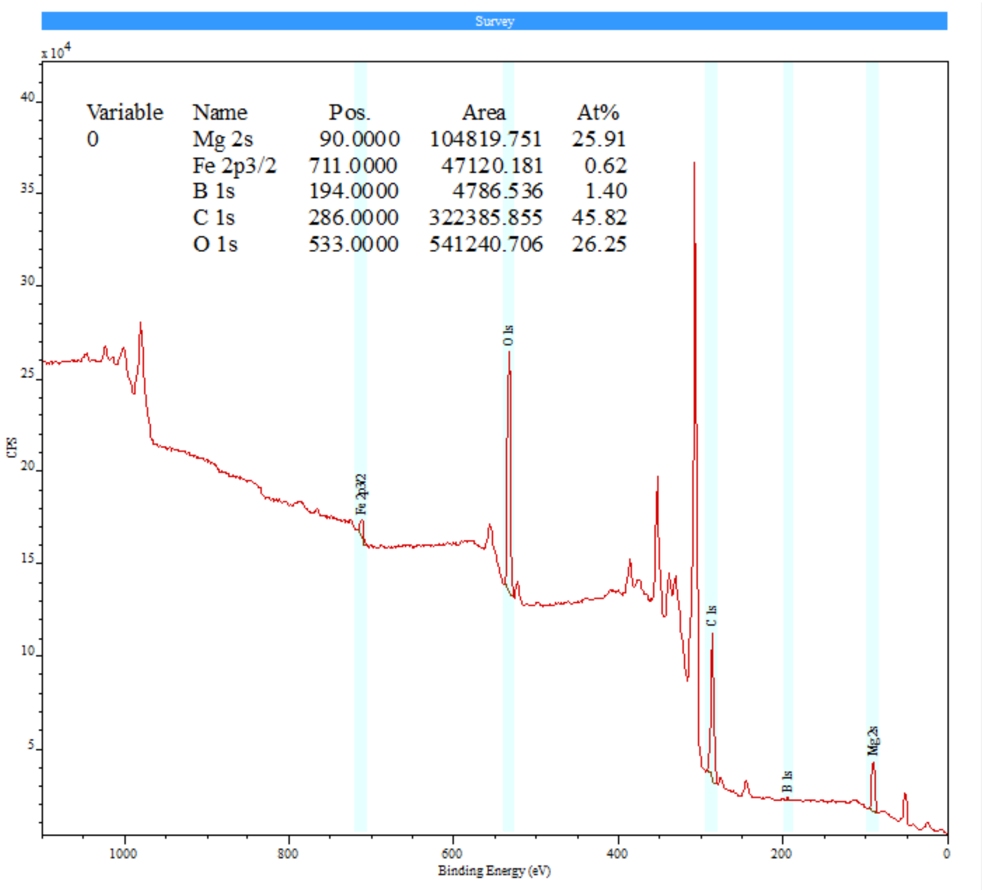

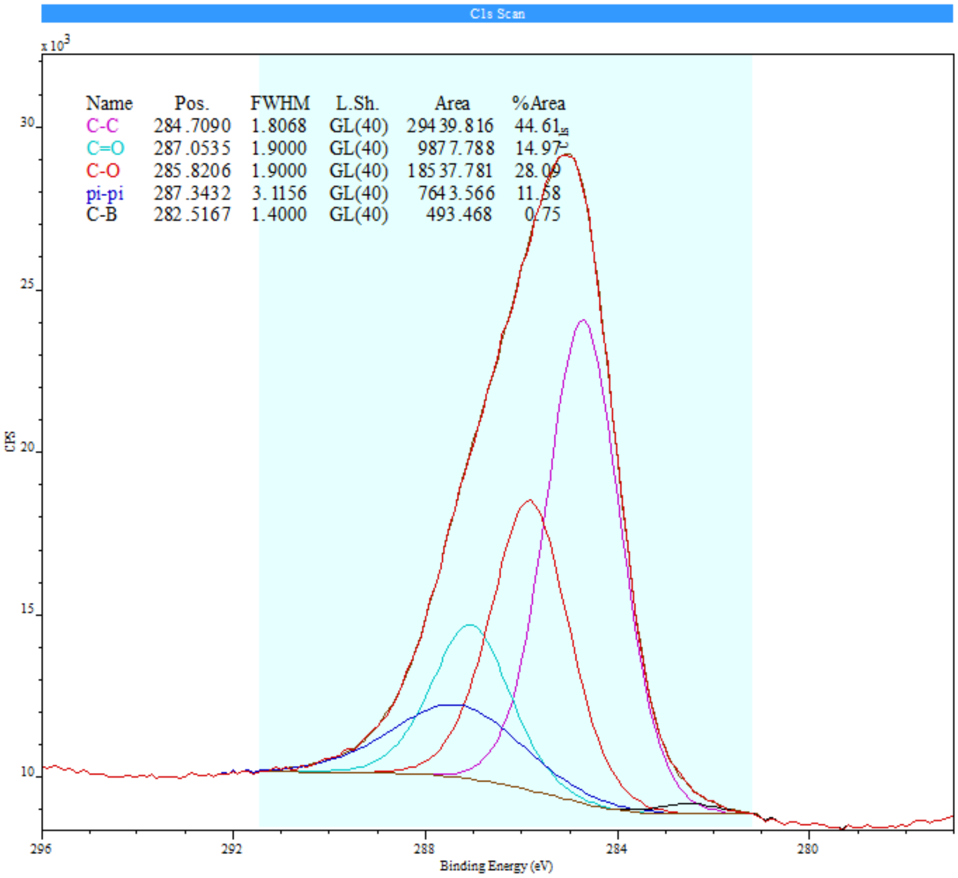
C1s Scan
x 10^3
Name Pos. FWHM L.Sh. Area %Area
C-C 284.7090 1.8068 GL(40) 29439.816 44.61
C=O 287.0535 1.9000 GL(40) 9877.788 14.97
C-O 285.8206 1.9000 GL(40) 18537.781 28.09
pi-pi 287.3432 3.1156 GL(40) 7643.566 11.58
C-B 282.5167 1.4000 GL(40) 493.468 0.75
CPS
30
25
20
15
10
296
292
288
284
280
Binding Energy (eV)

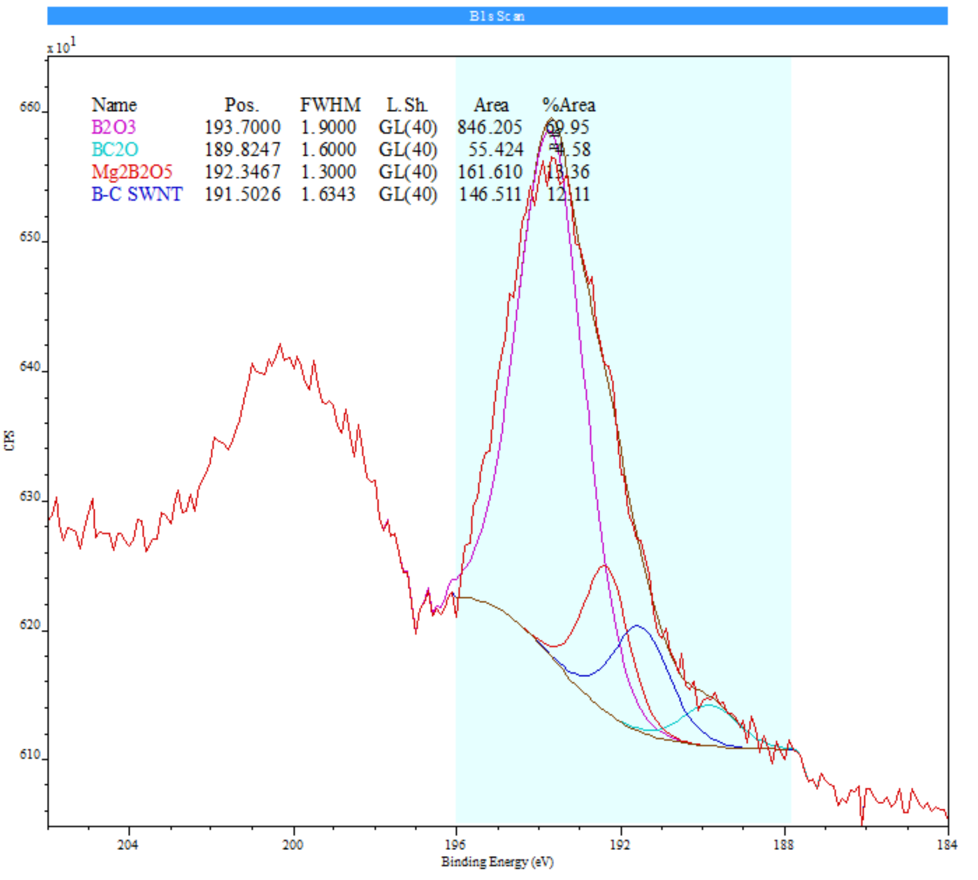
B1s Scan
x 10^1
Name Pos. FWHM L.Sh. Area %Area
B2O3 193.7000 1.9000 GL(40) 846.205 69.95
BC2O 189.8247 1.6000 GL(40) 55.424 4.58
Mg2B2O5 192.3467 1.3000 GL(40) 161.610 13.36
B-C SWNT 191.5026 1.6343 GL(40) 146.511 12.11
CPS
660
650
640
630
620
610
204
200
196
192
188
184
Binding Energy (eV)

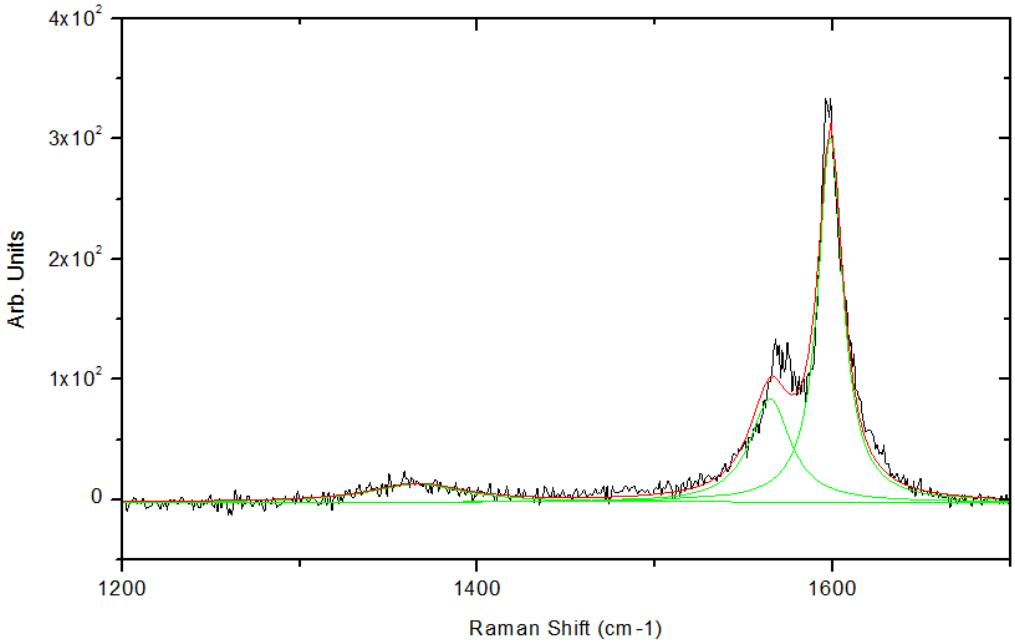
4x10^2
3x10^2
2x10^2
1x10^2
0
Arb. Units
1200
1400
1600
Raman Shift (cm-1)

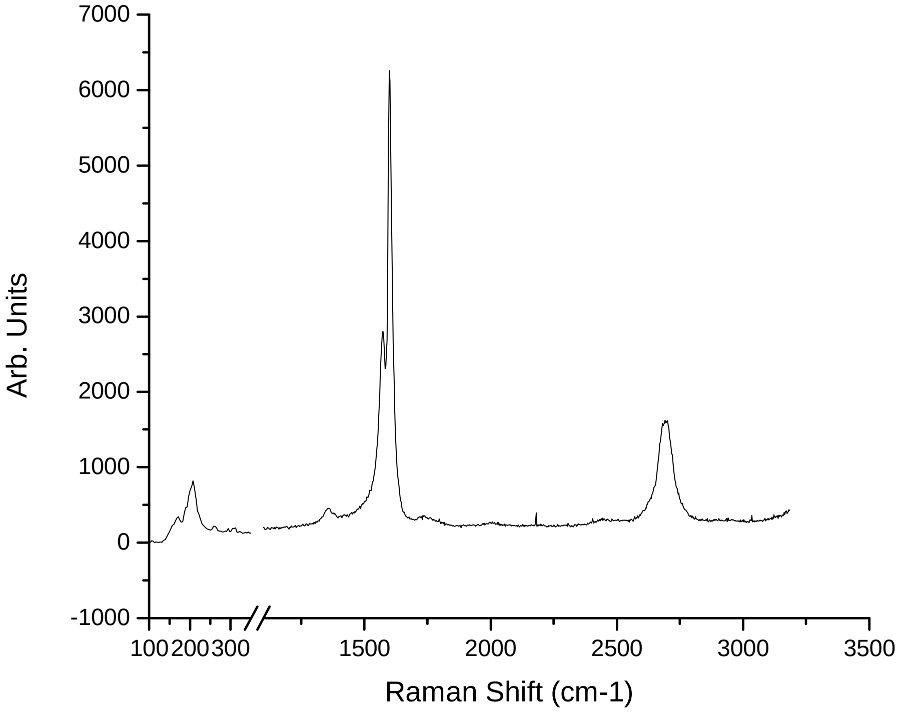
7000
6000
5000
4000
3000
2000
1000
0
-1000
Arb. Units
100 200 300
1500
2000
2500
3000
3500
Raman Shift (cm-1)

**Experiment Run 7:**

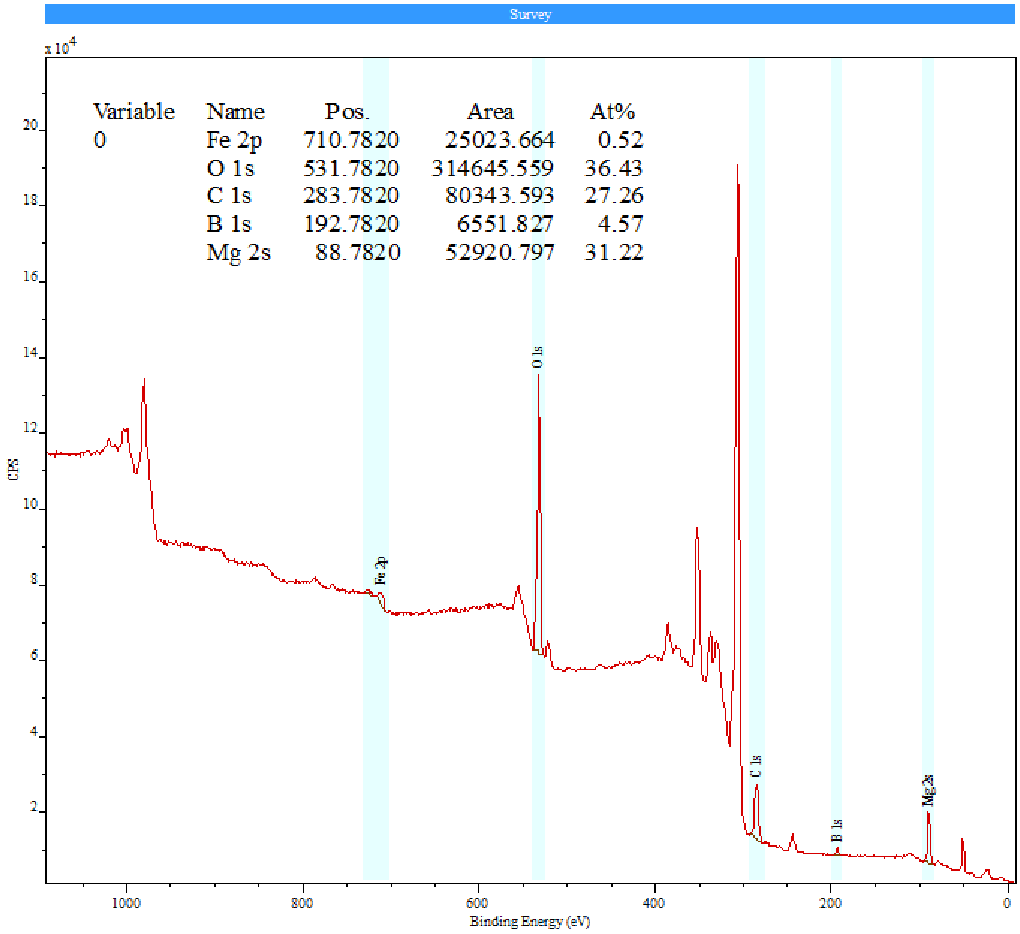

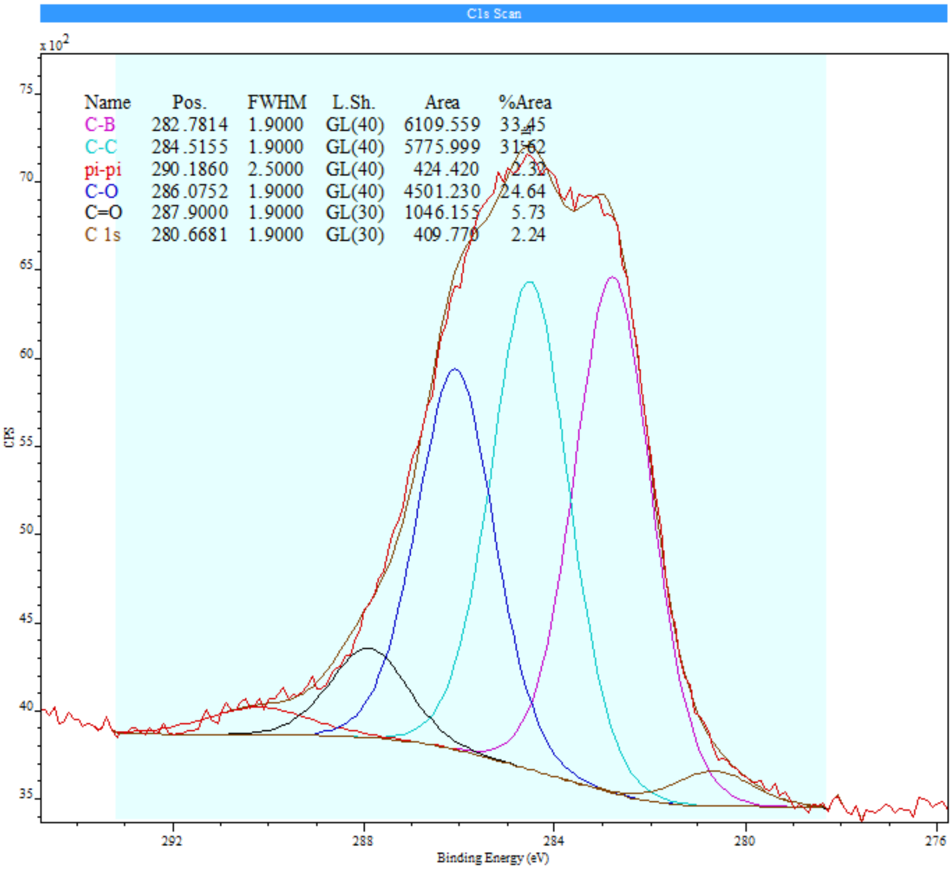
C1s Scan
x 10^2
Name Pos. FWHM L.Sh. Area %Area
C-B 282.7814 1.9000 GL(40) 6109.559 33.45
C-C 284.5155 1.9000 GL(40) 5775.999 31.62
pi-pi 290.1860 2.5000 GL(40) 424.420 2.32
C-O 286.0752 1.9000 GL(40) 4501.230 24.64
C=O 287.9000 1.9000 GL(30) 1046.155 5.73
C 1s 280.6681 1.9000 GL(30) 409.770 2.24
CPS
Binding Energy (eV)

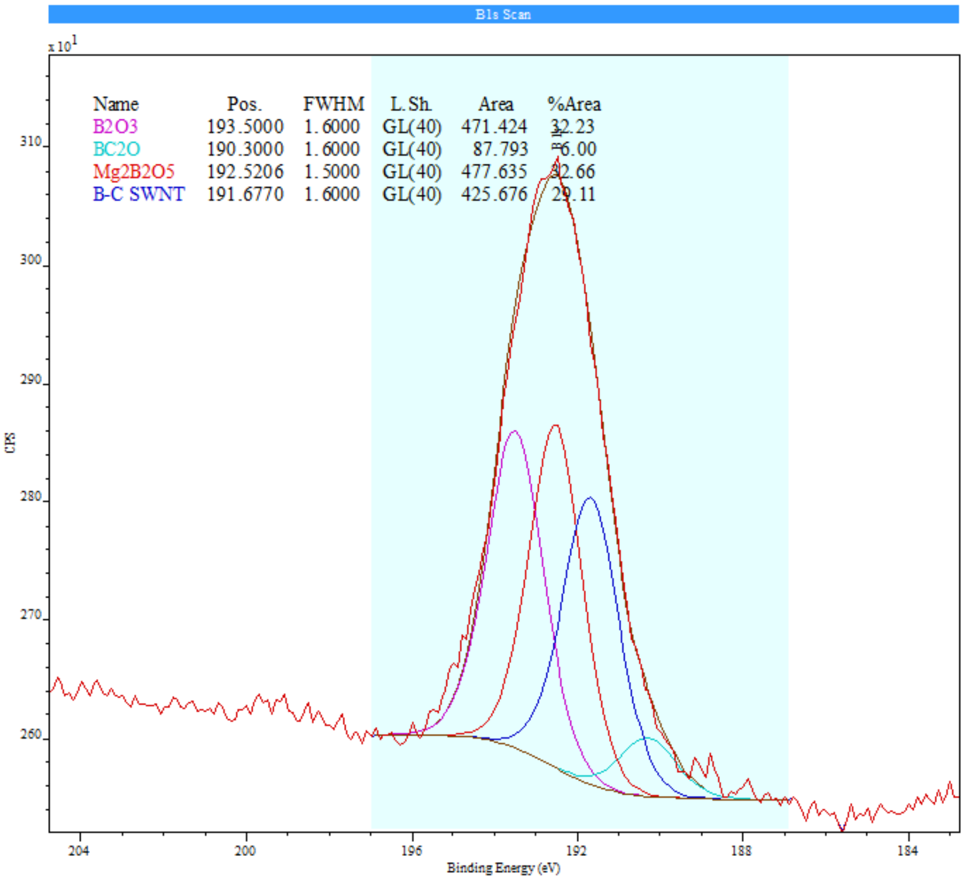
B1s Scan
x 10^1
Name Pos. FWHM L.Sh. Area %Area
B2O3 193.5000 1.6000 GL(40) 471.424 32.23
BC2O 190.3000 1.6000 GL(40) 87.793 6.00
Mg2B2O5 192.5206 1.5000 GL(40) 477.635 32.66
B-C SWNT 191.6770 1.6000 GL(40) 425.676 29.11
CPS
Binding Energy (eV)

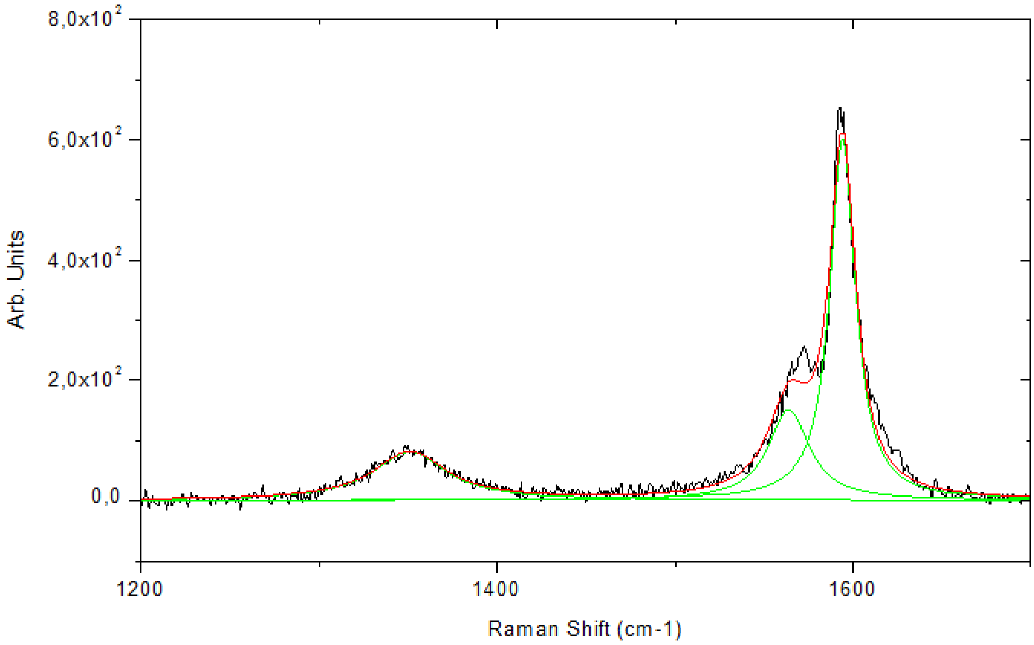
8,0x10²
6,0x10²
4,0x10²
2,0x10²
0,0
Arb. Units
1200
1400
1600
Raman Shift (cm-1)

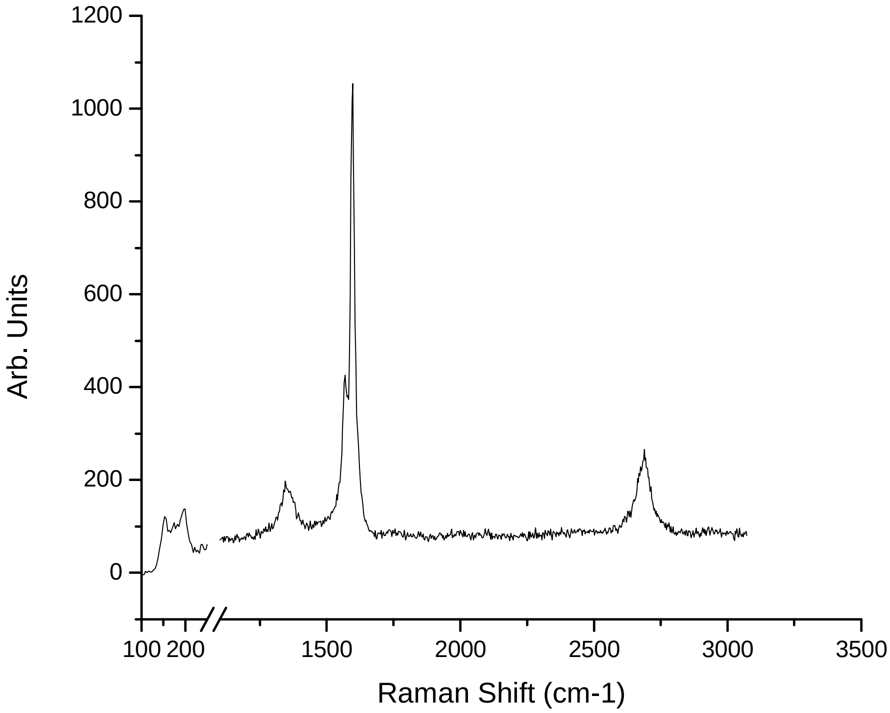
1200
1000
800
600
400
200
0
Arb. Units
100 200
1500
2000
2500
3000
3500
Raman Shift (cm-1)

**Experiment Run 8:**

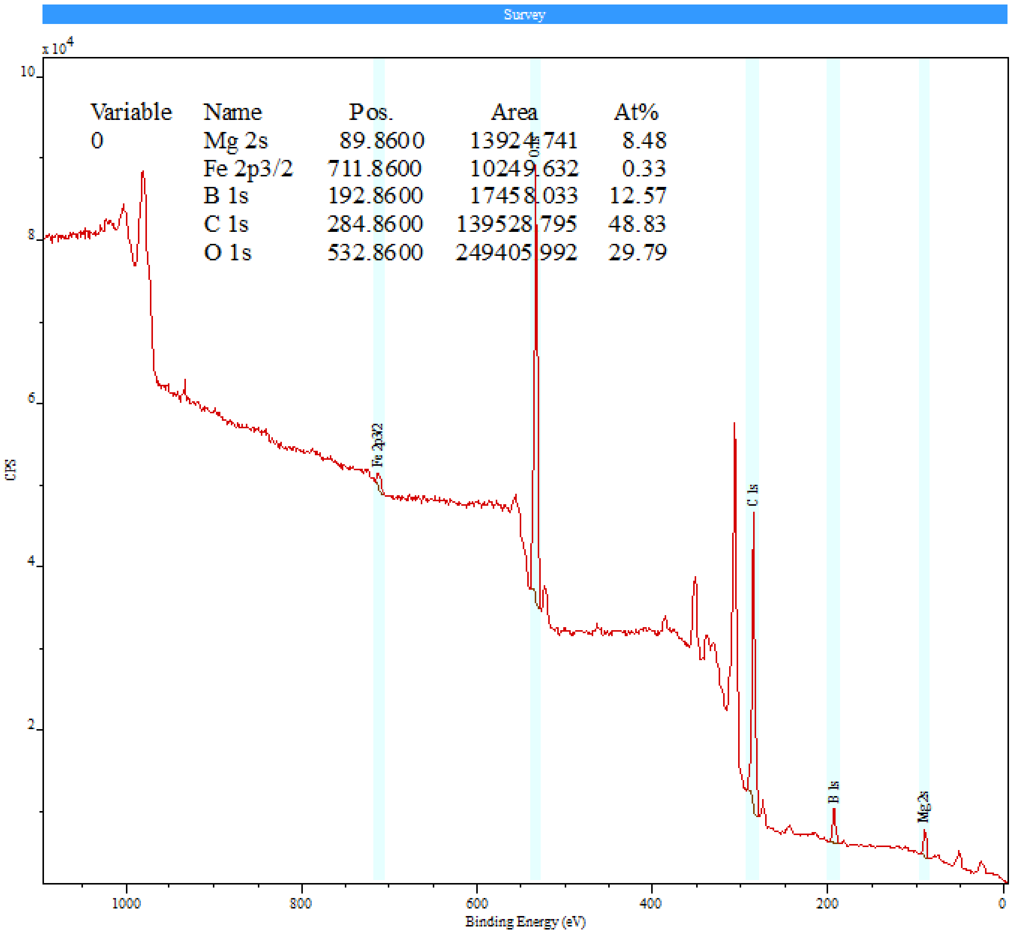

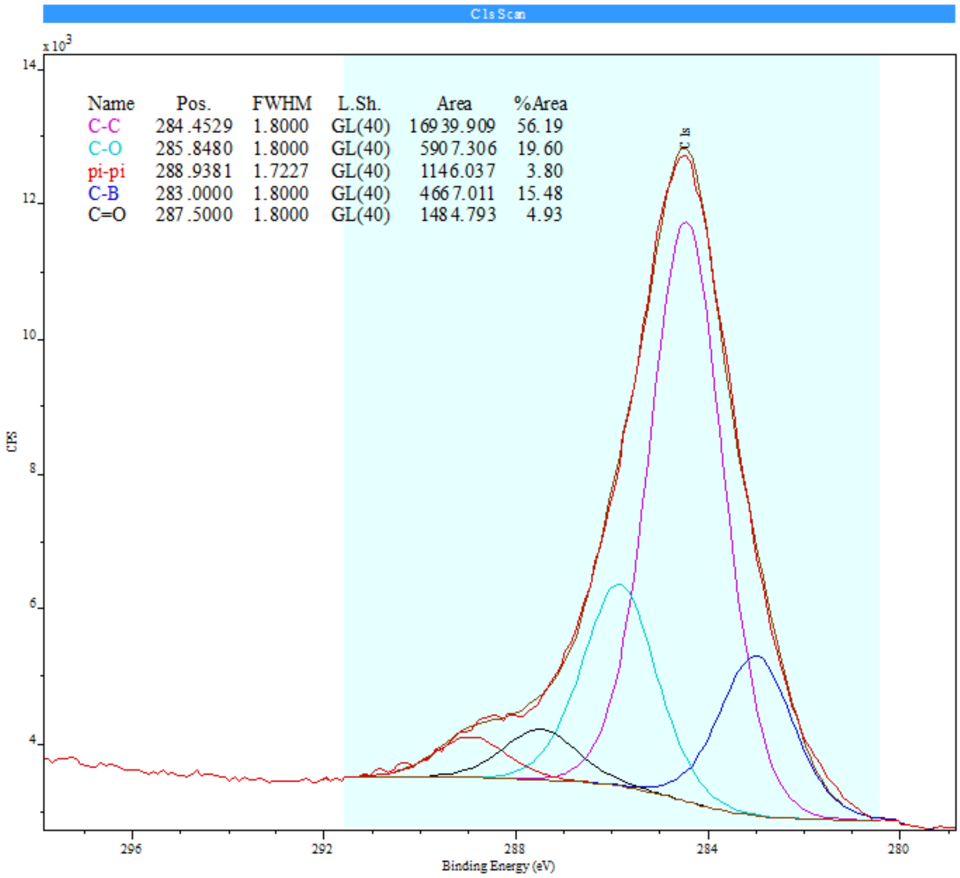


No B1s spectrum was acquired for this sample.

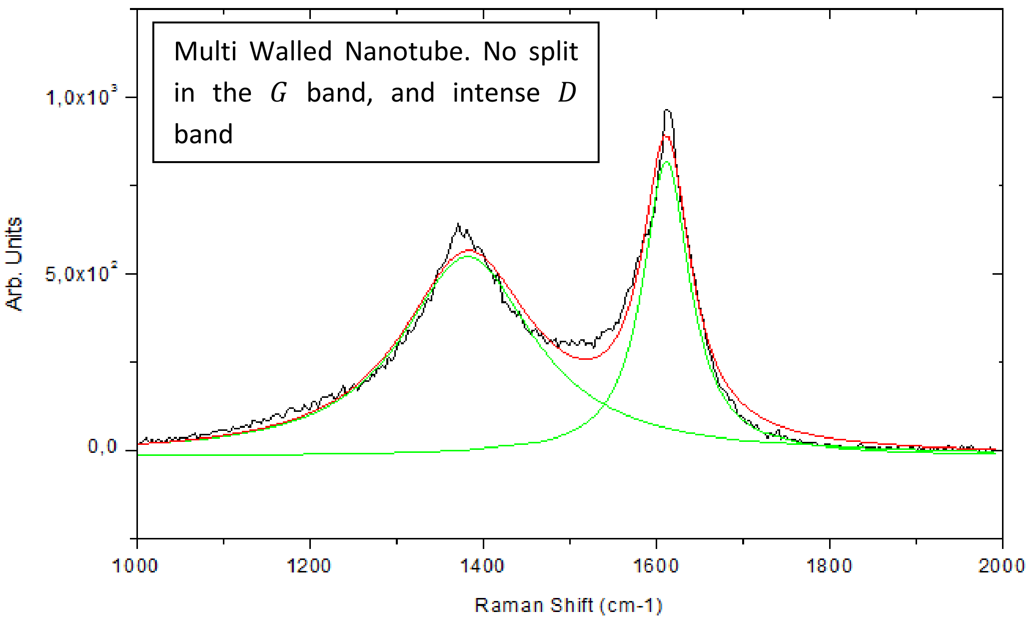

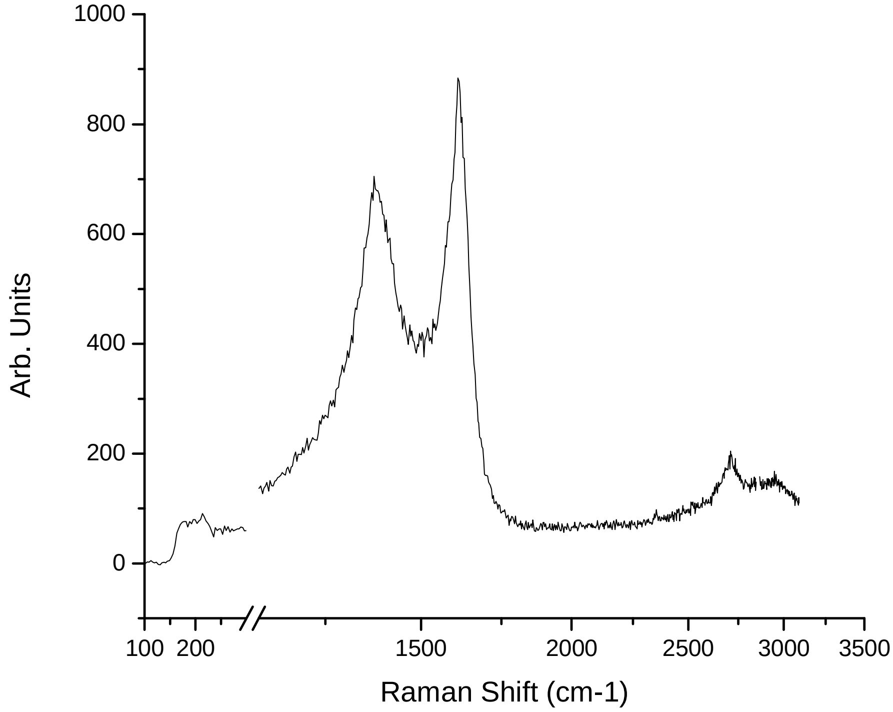


**Experiment Run 9:**

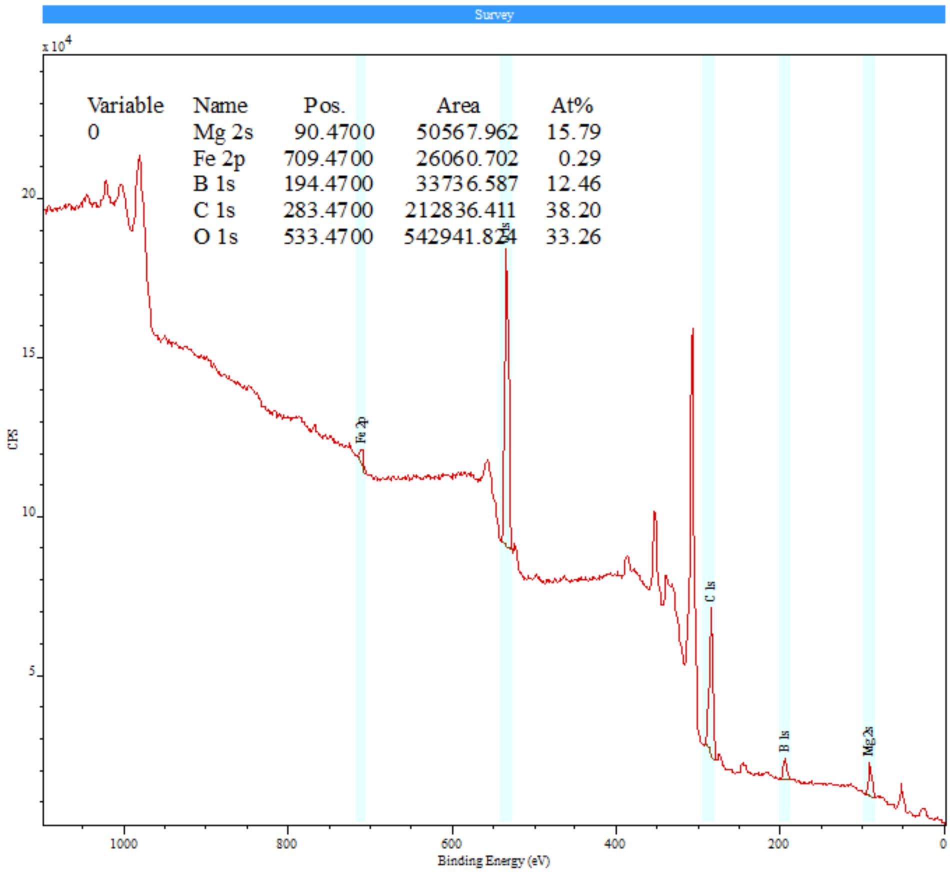

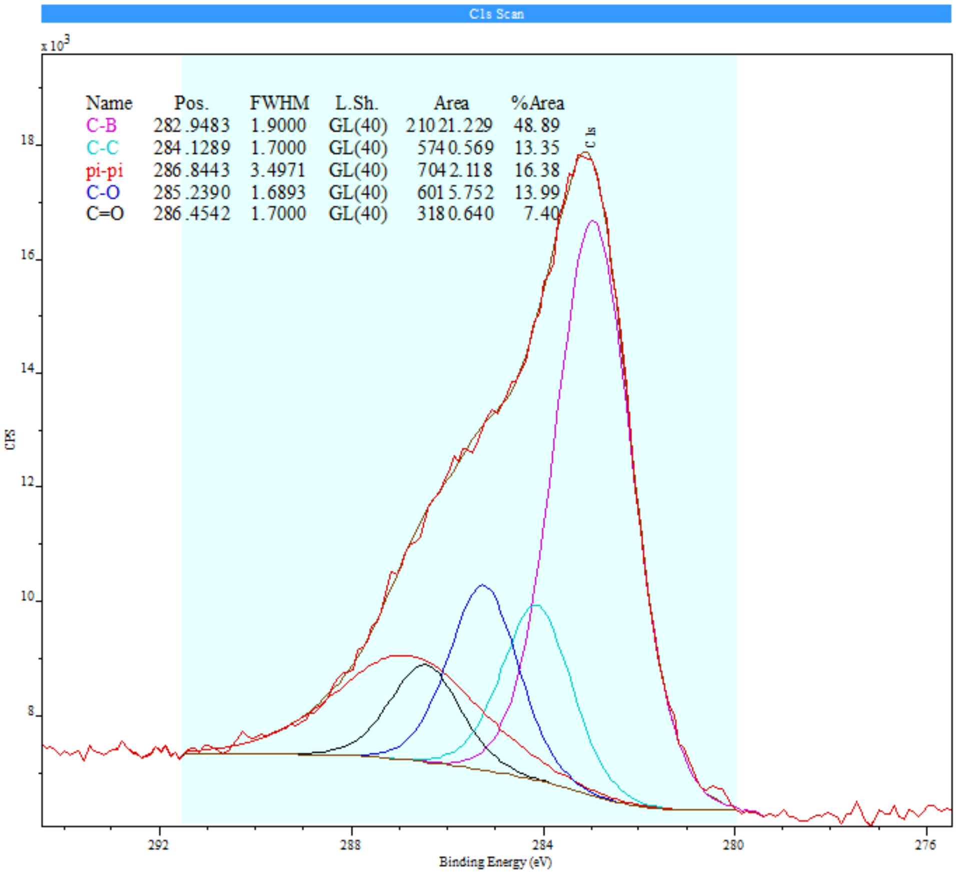
C1s Scan
x 10^3
Name Pos. FWHM L.Sh. Area %Area
C-B 282.9483 1.9000 GL(40) 21021.229 48.89
C-C 284.1289 1.7000 GL(40) 5740.569 13.35
pi-pi 286.8443 3.4971 GL(40) 7042.118 16.38
C-O 285.2390 1.6893 GL(40) 6015.752 13.99
C=O 286.4542 1.7000 GL(40) 3180.640 7.40
C 1s
CPS
18
16
14
12
10
8
292
288
284
280
276
Binding Energy (eV)

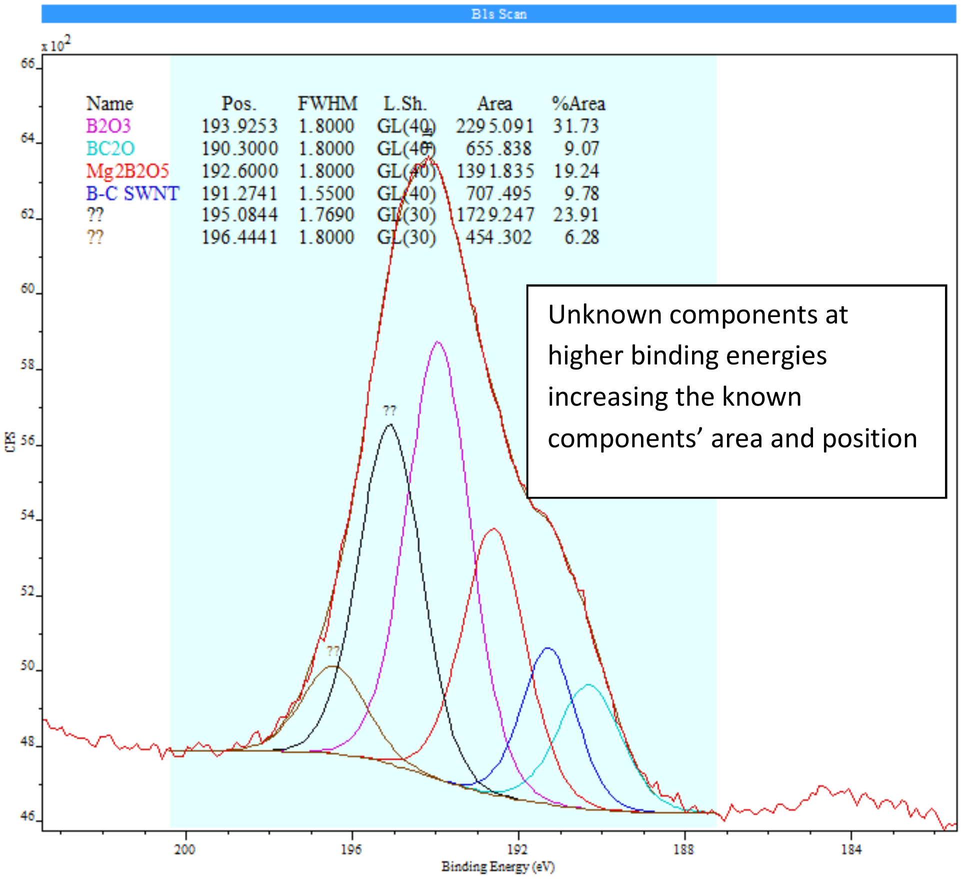
B1s Scan
x 10^2
Name Pos. FWHM L.Sh. Area %Area
B2O3 193.9253 1.8000 GL(40) 2295.091 31.73
BC2O 190.3000 1.8000 GL(40) 655.838 9.07
Mg2B2O5 192.6000 1.8000 GL(40) 1391.835 19.24
B-C SWNT 191.2741 1.5500 GL(40) 707.495 9.78
?? 195.0844 1.7690 GL(30) 1729.247 23.91
?? 196.4441 1.8000 GL(30) 454.302 6.28
Unknown components at higher binding energies increasing the known components' area and position
??
??
CPS
66
64
62
60
58
56
54
52
50
48
46
200
196
192
188
184
Binding Energy (eV)

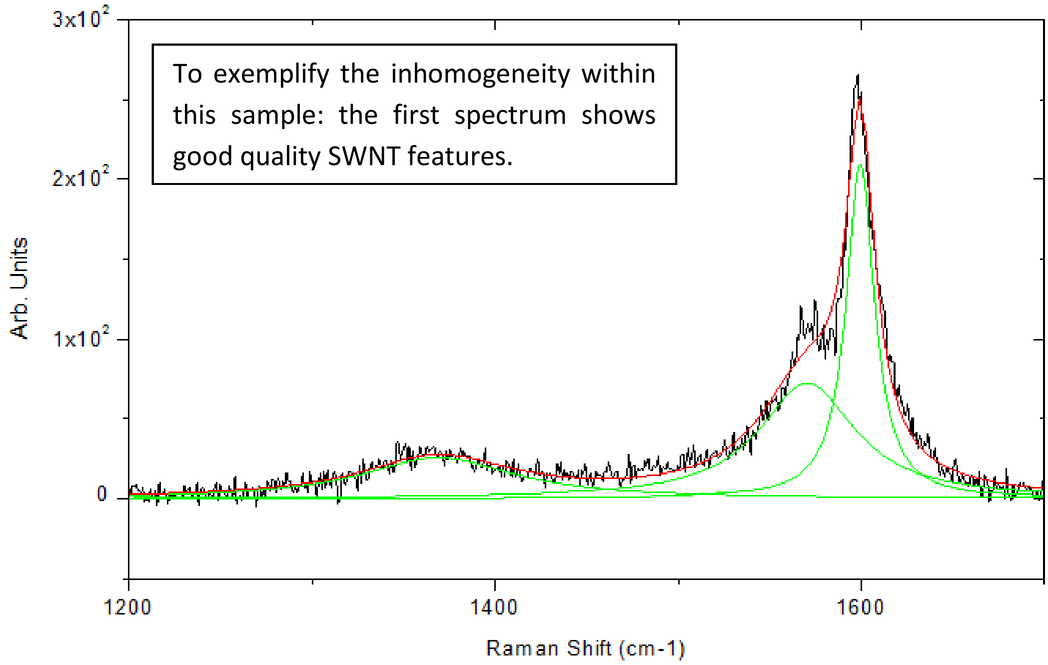
To exemplify the inhomogeneity within this sample: the first spectrum shows good quality SWNT features.
3x10²
2x10²
1x10²
0
Arb. Units
1200
1400
1600
Raman Shift (cm-1)

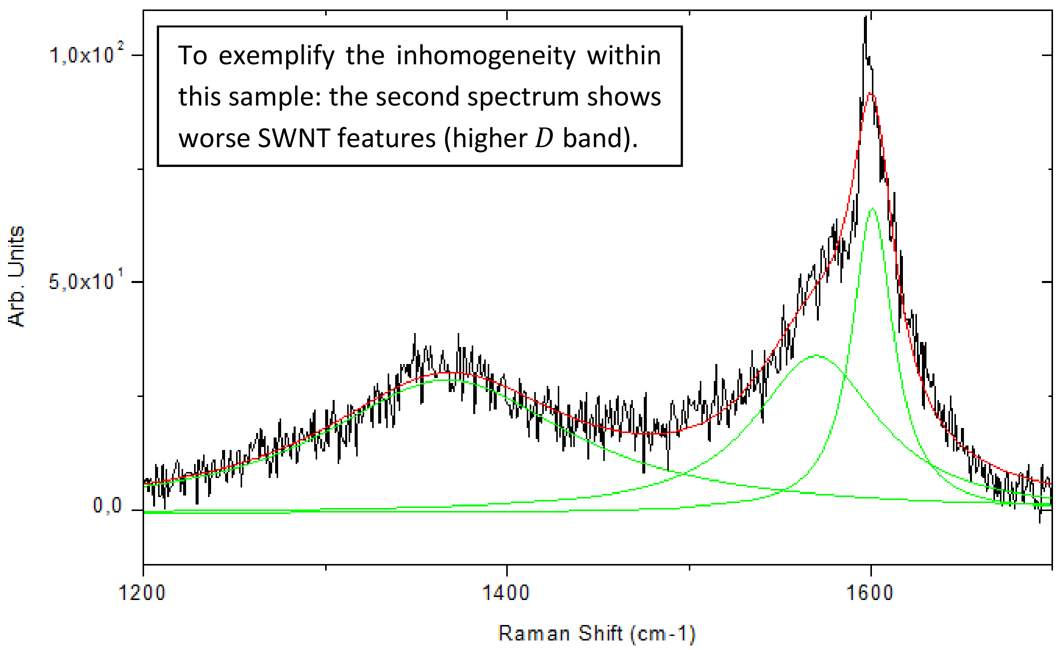
To exemplify the inhomogeneity within this sample: the second spectrum shows worse SWNT features (higher D band).
1,0x10²
5,0x10¹
0,0
Arb. Units
1200
1400
1600
Raman Shift (cm-1)

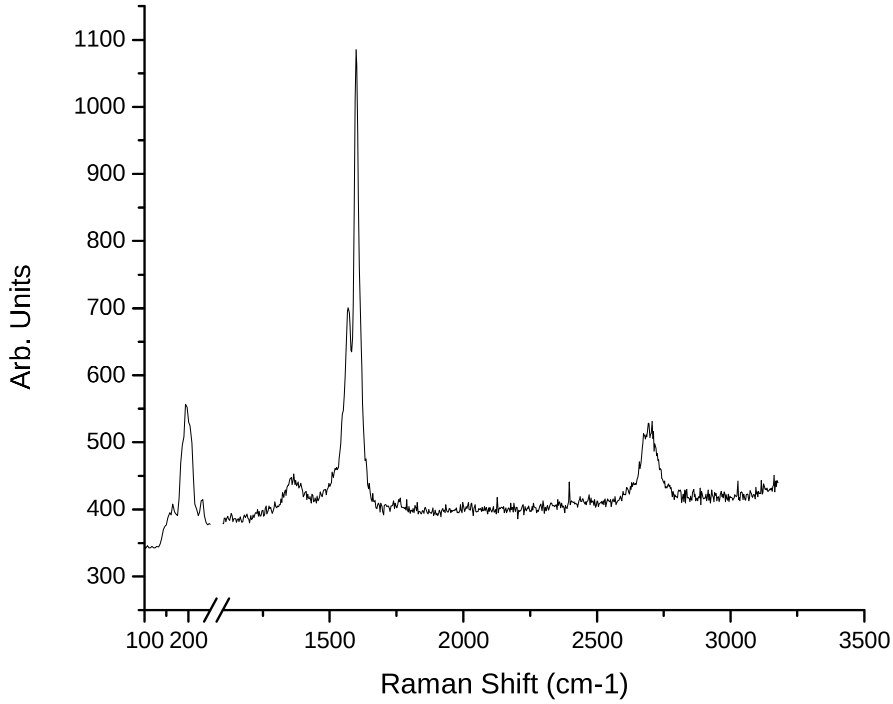


**Experiment Run 10:**

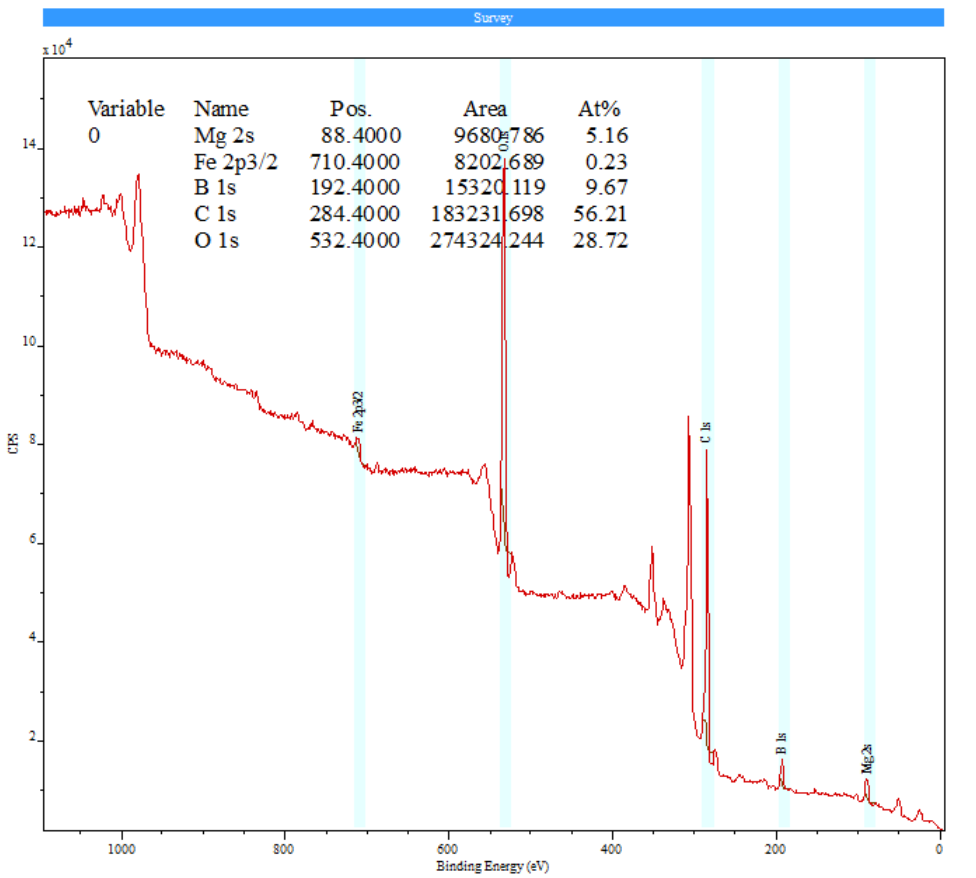

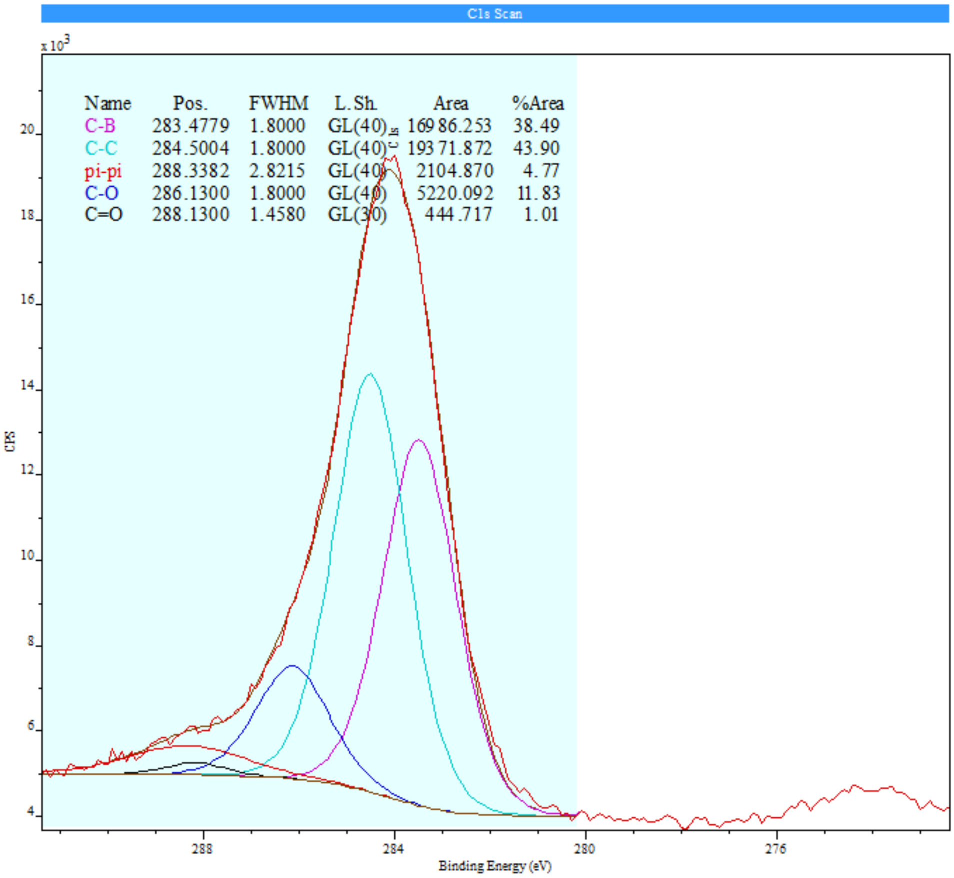
C1s Scan
x 10^3
Name Pos. FWHM L.Sh. Area %Area
C-B 283.4779 1.8000 GL(40) 16986.253 38.49
C-C 284.5004 1.8000 GL(40) 19371.872 43.90
pi-pi 288.3382 2.8215 GL(40) 2104.870 4.77
C-O 286.1300 1.8000 GL(40) 5220.092 11.83
C=O 288.1300 1.4580 GL(30) 444.717 1.01
CPS
Binding Energy (eV)

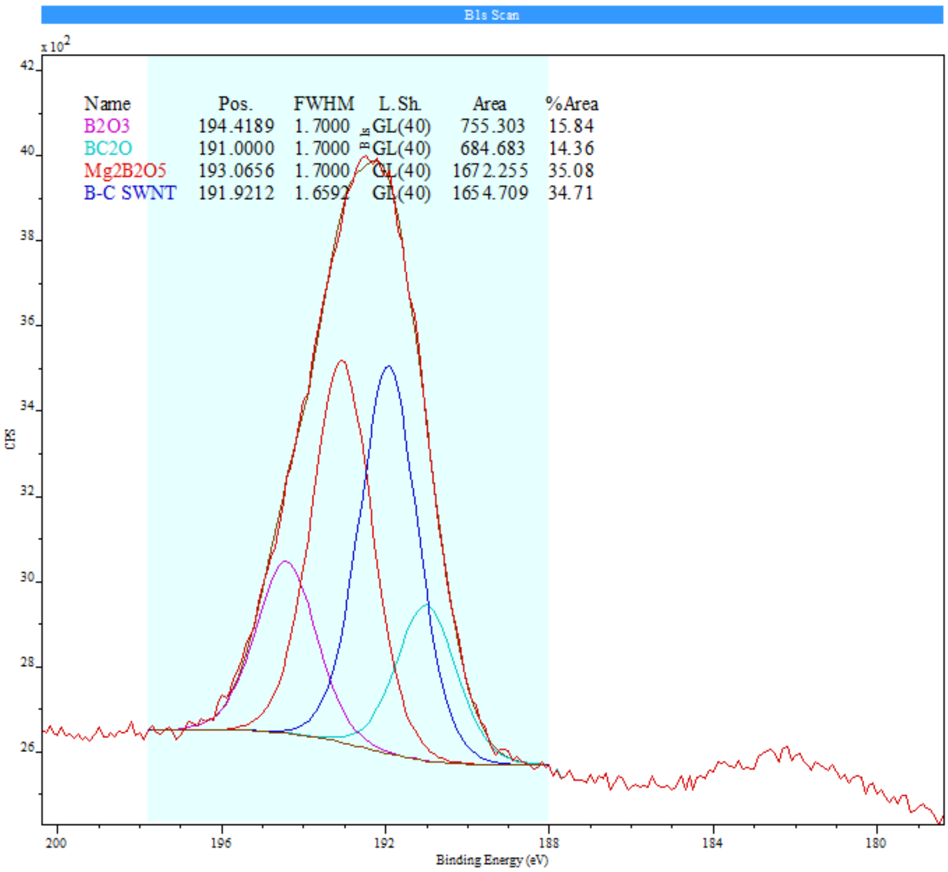
B1s Scan
x 10^2
Name Pos. FWHM L.Sh. Area %Area
B2O3 194.4189 1.7000 GL(40) 755.303 15.84
BC2O 191.0000 1.7000 GL(40) 684.683 14.36
Mg2B2O5 193.0656 1.7000 GL(40) 1672.255 35.08
B-C SWNT 191.9212 1.6592 GL(40) 1654.709 34.71
CPS
Binding Energy (eV)

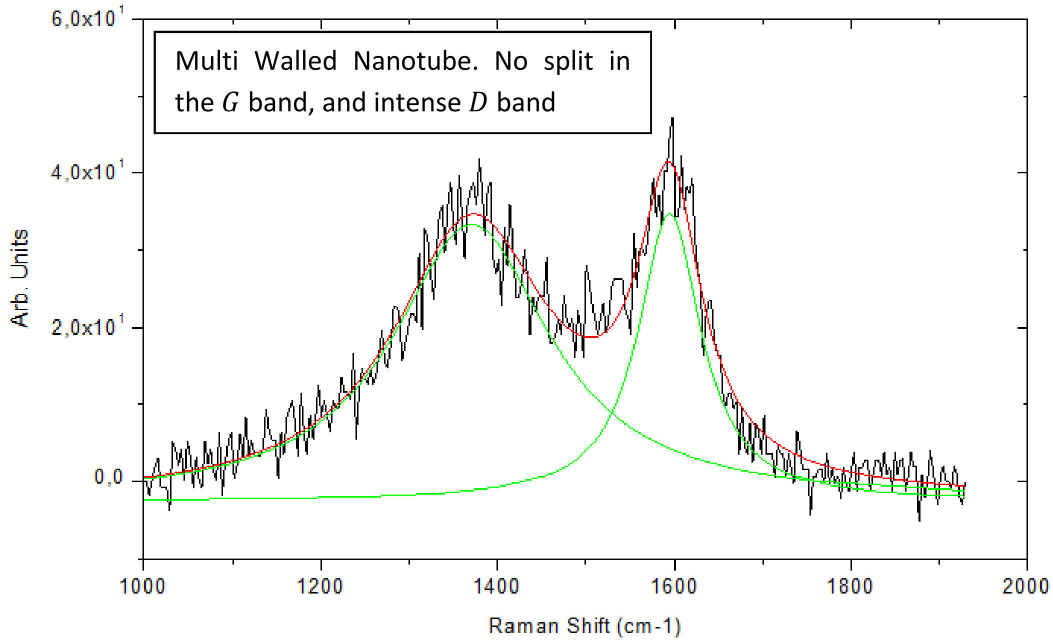




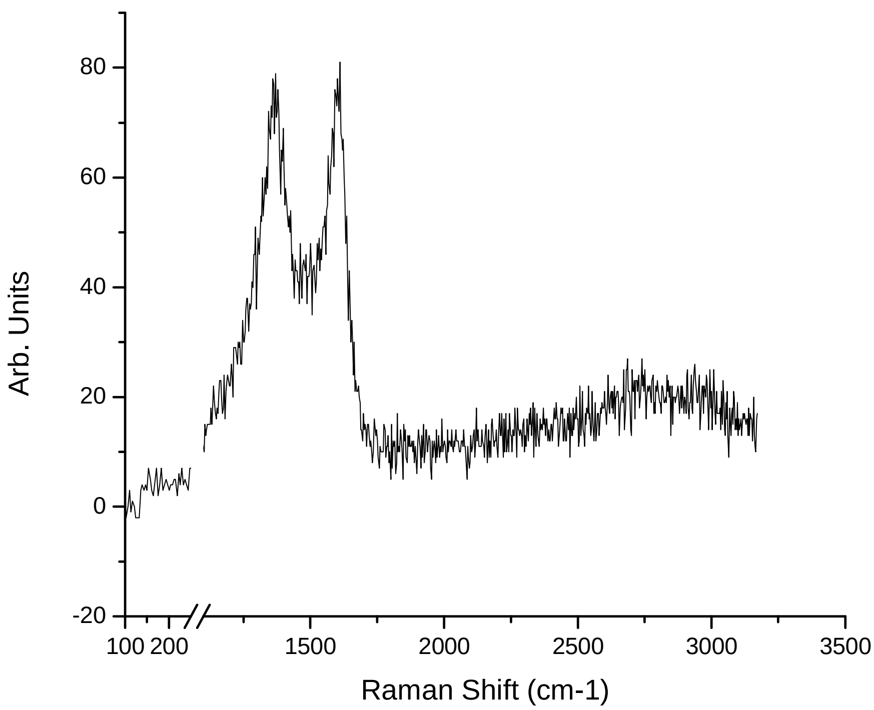


**Experiment Run 11:**

This experiment does not have XPS recorded.

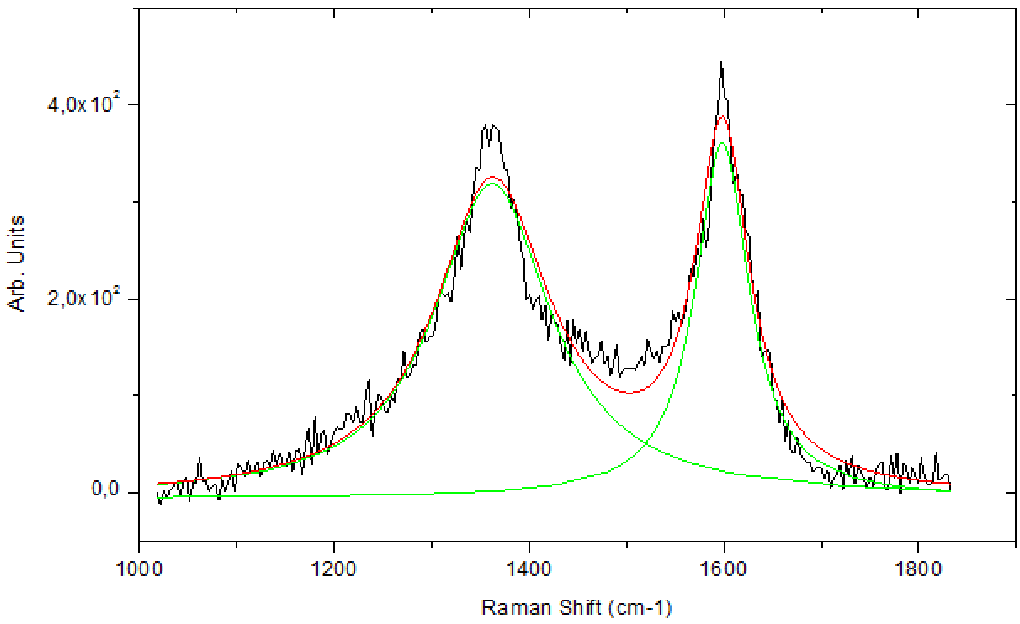
4,0x10²
2,0x10²
0,0
Arb. Units
1000
1200
1400
1600
1800
Raman Shift (cm-1)

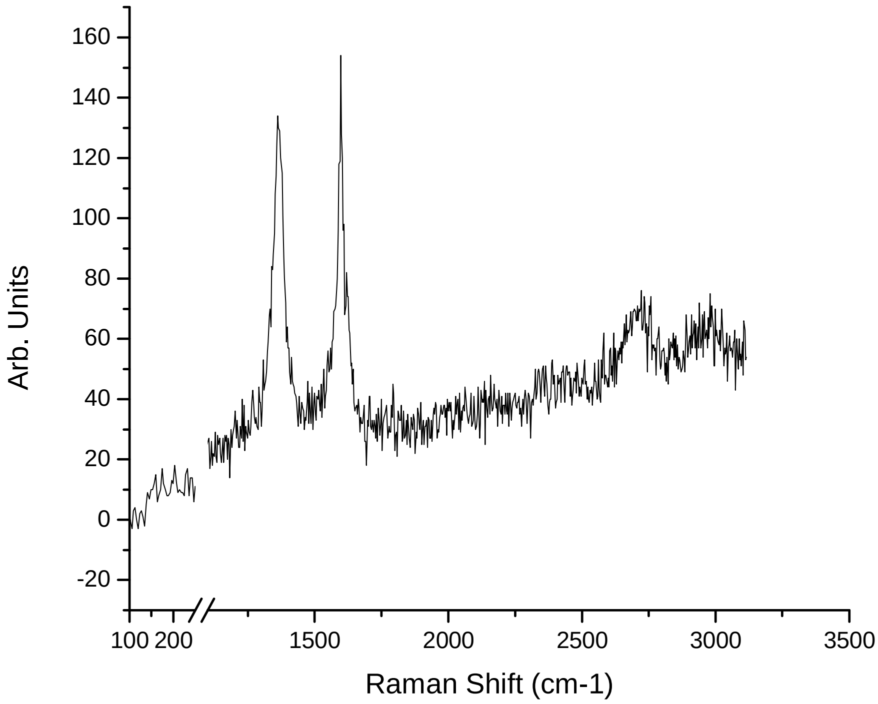
160
140
120
100
80
60
40
20
0
-20
Arb. Units
100 200
1500
2000
2500
3000
3500
Raman Shift (cm-1)

**Experiment Run 12:**

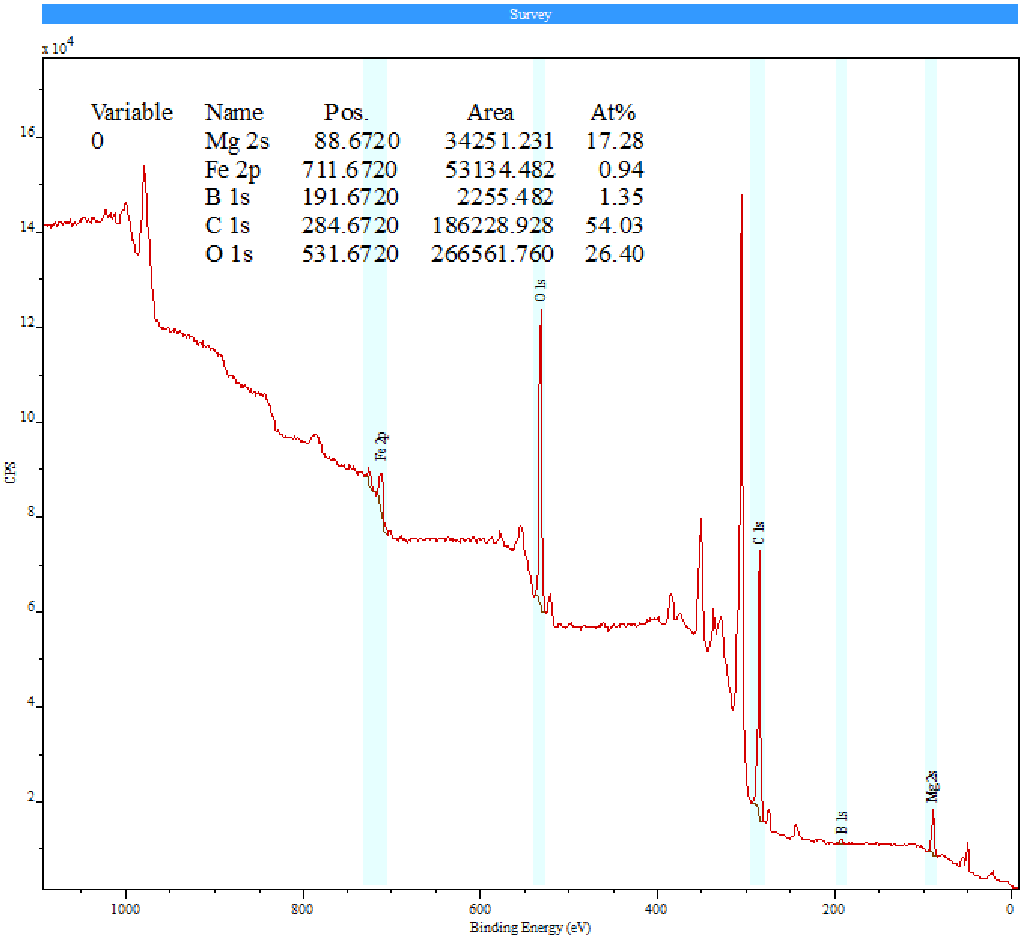

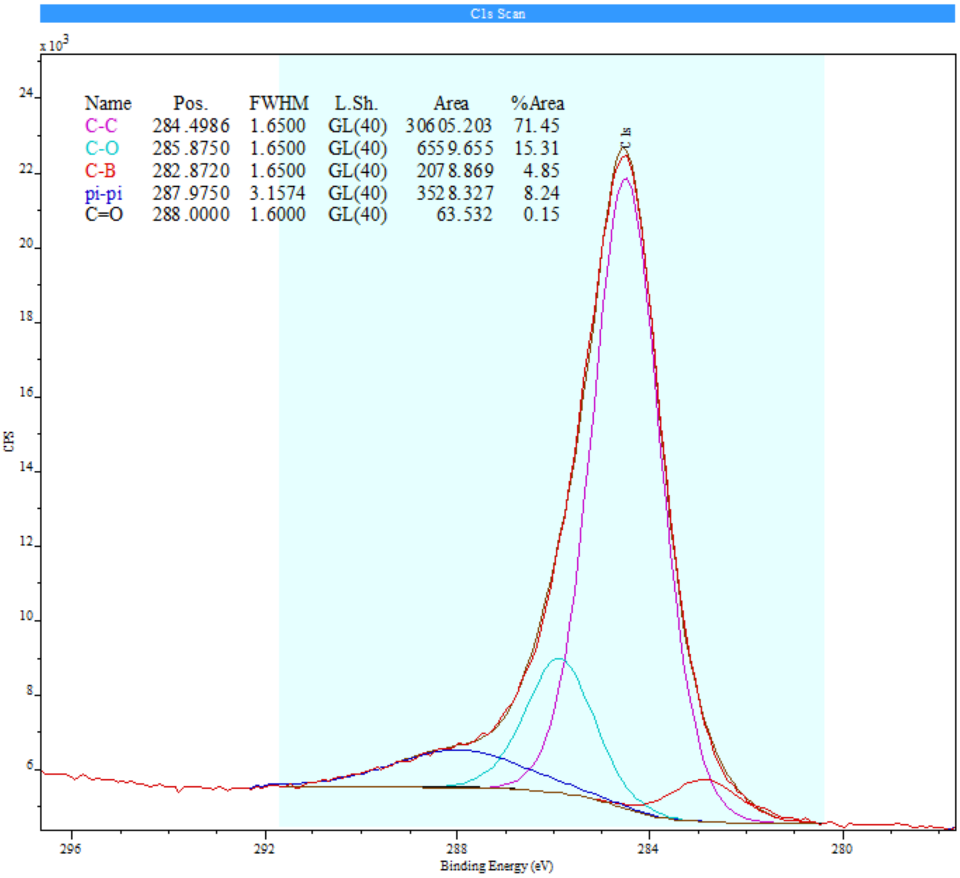
C1s Scan
x 10^3
Name Pos. FWHM L.Sh. Area %Area
C-C 284.4986 1.6500 GL(40) 30605.203 71.45
C-O 285.8750 1.6500 GL(40) 6559.655 15.31
C-B 282.8720 1.6500 GL(40) 2078.869 4.85
pi-pi 287.9750 3.1574 GL(40) 3528.327 8.24
C=O 288.0000 1.6000 GL(40) 63.532 0.15
C 1s
CPS
Binding Energy (eV)

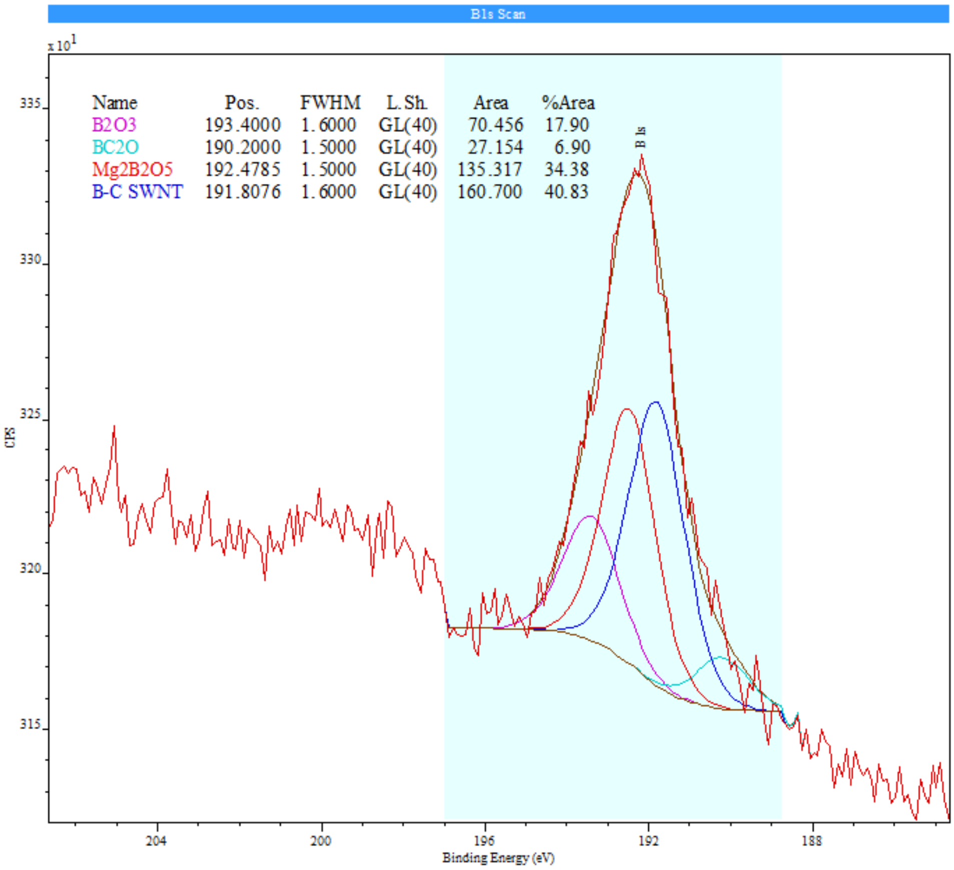
B1s Scan
x 10^1
Name Pos. FWHM L.Sh. Area %Area
B2O3 193.4000 1.6000 GL(40) 70.456 17.90
BC2O 190.2000 1.5000 GL(40) 27.154 6.90
Mg2B2O5 192.4785 1.5000 GL(40) 135.317 34.38
B-C SWNT 191.8076 1.6000 GL(40) 160.700 40.83
B 1s
CPS
Binding Energy (eV)

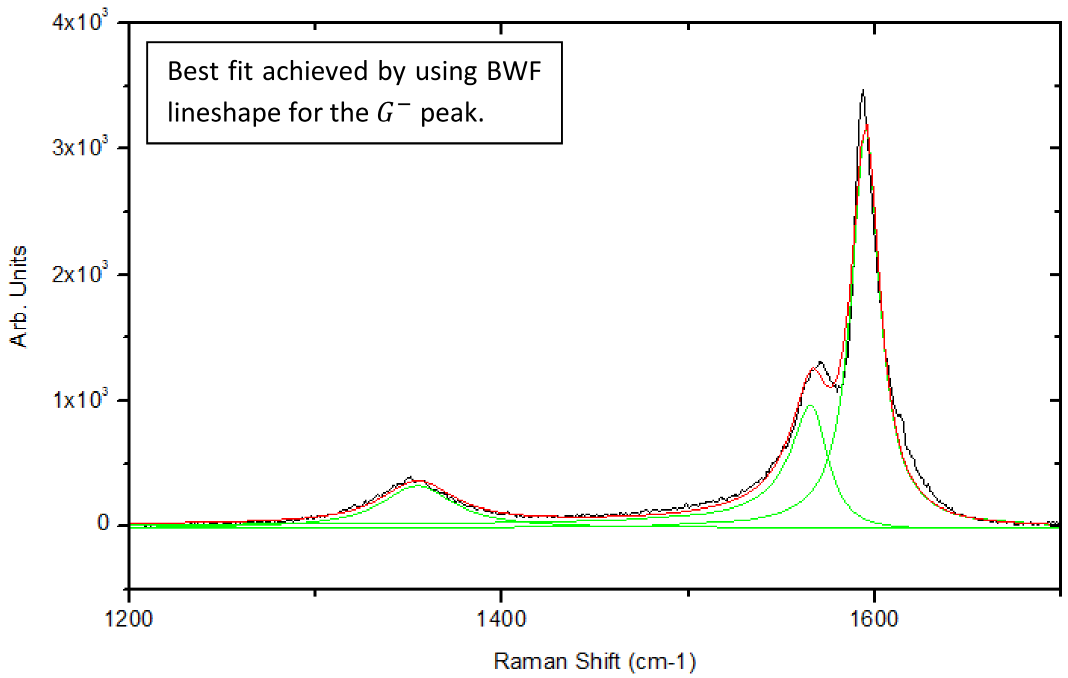
Best fit achieved by using BWF lineshape for the $G^-$ peak.
4x10³
3x10³
2x10³
1x10³
0
Arb. Units
1200
1400
1600
Raman Shift (cm-1)

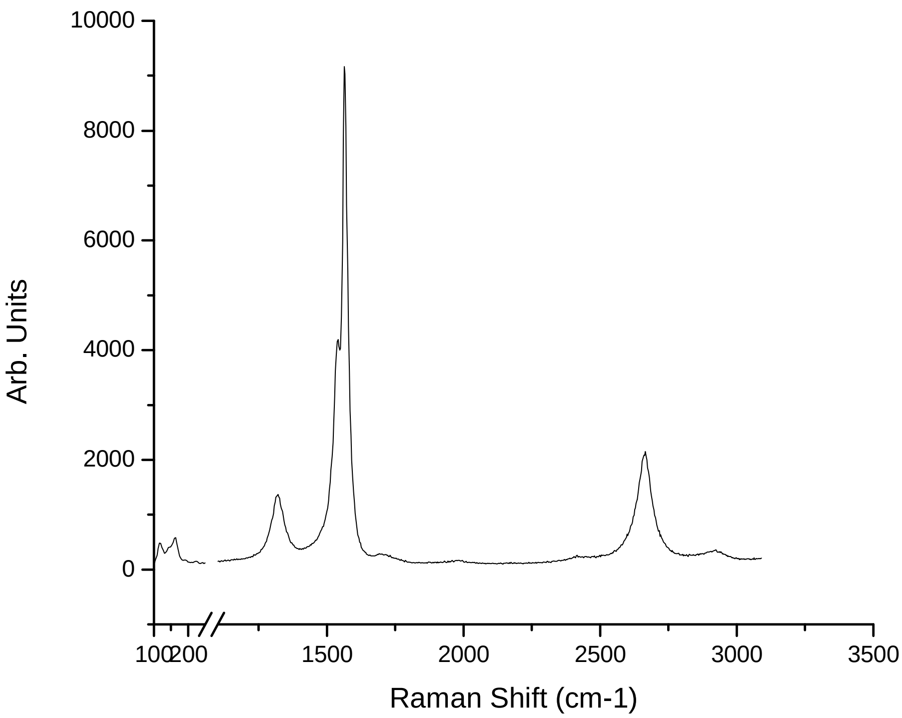
10000
8000
6000
4000
2000
0
Arb. Units
100
200
1500
2000
2500
3000
3500
Raman Shift (cm-1)

**Experiment Run 13:**

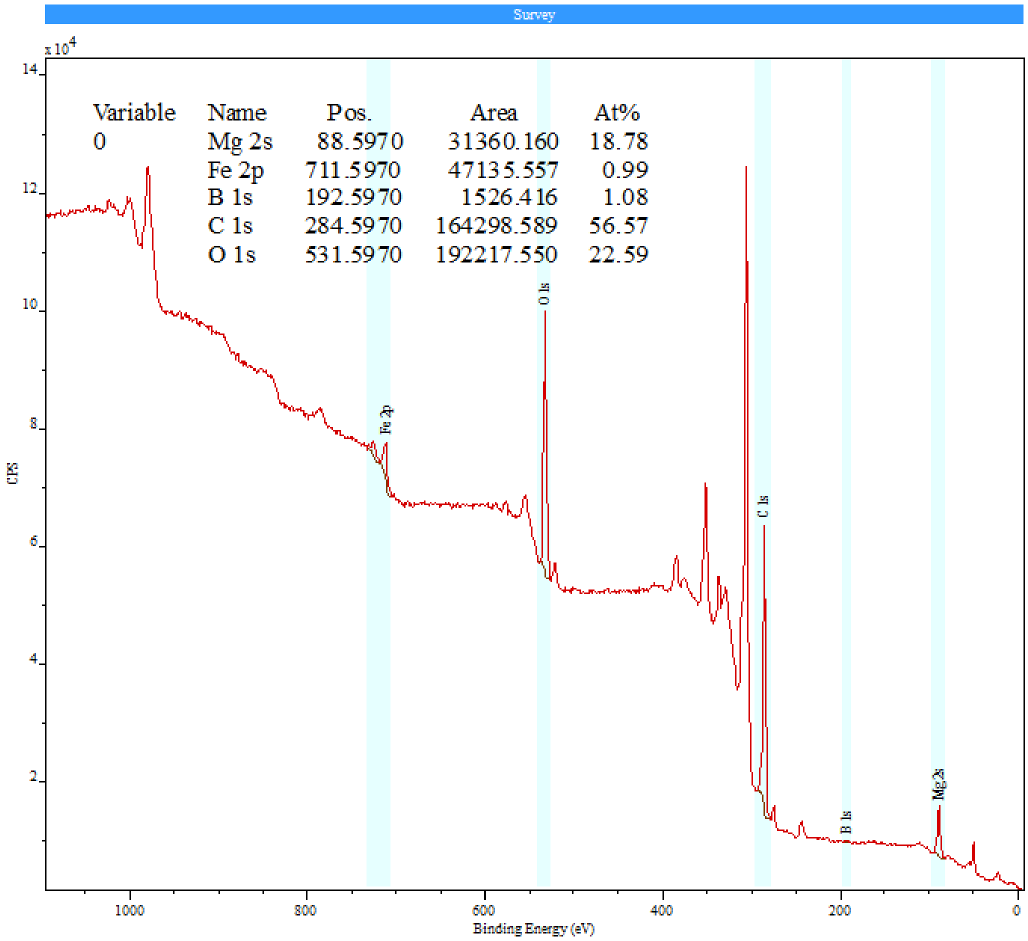

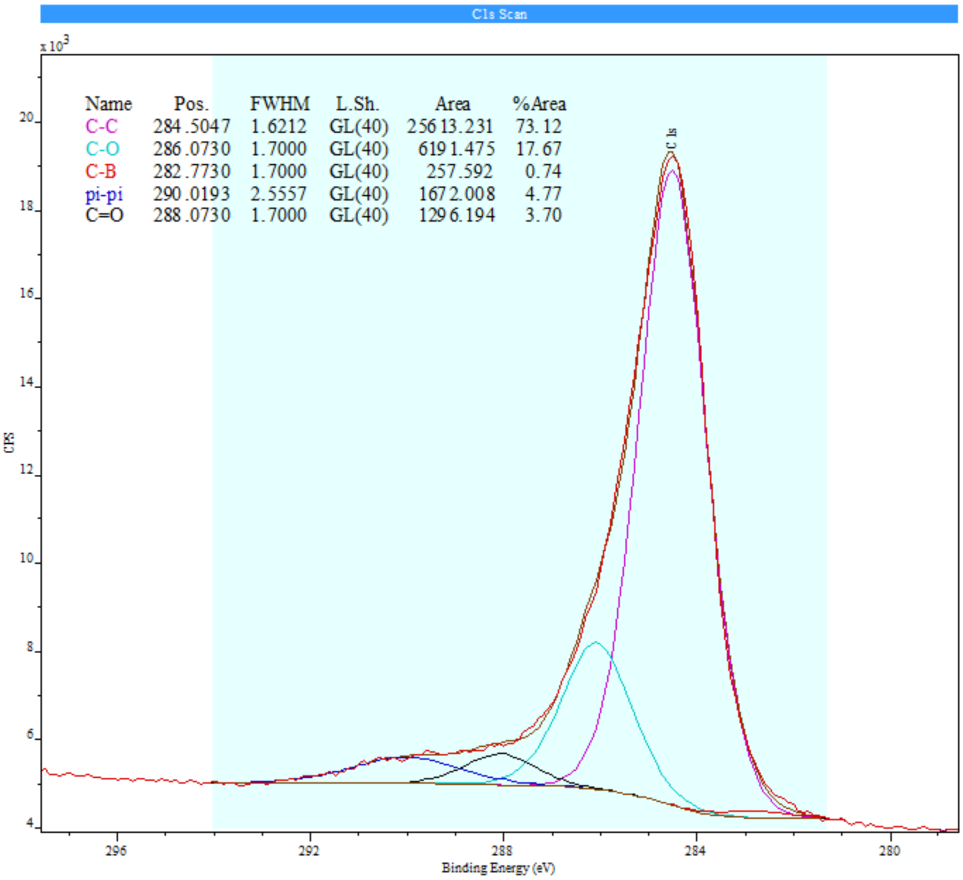
C1s Scan
x 10^3
Name Pos. FWHM L.Sh. Area %Area
C-C 284.5047 1.6212 GL(40) 25613.231 73.12
C-O 286.0730 1.7000 GL(40) 6191.475 17.67
C-B 282.7730 1.7000 GL(40) 257.592 0.74
pi-pi 290.0193 2.5557 GL(40) 1672.008 4.77
C=O 288.0730 1.7000 GL(40) 1296.194 3.70
C 1s
CPS
Binding Energy (eV)

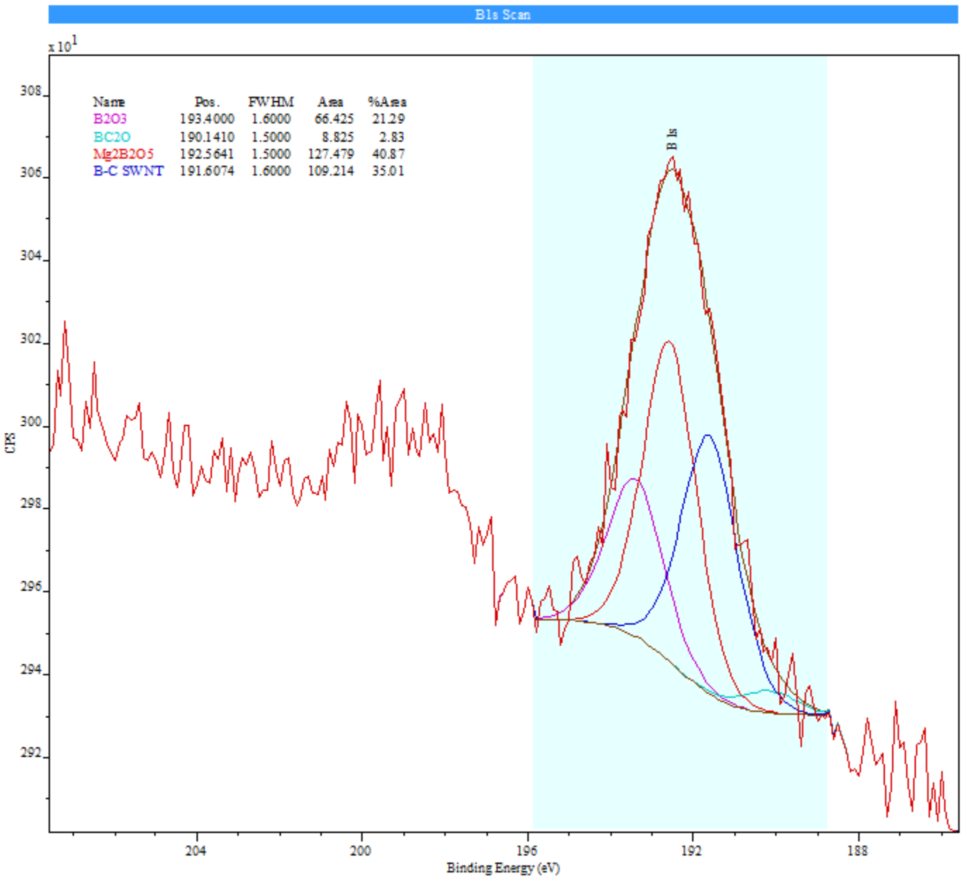
B1s Scan
x 10^1
Name Pos. FWHM Area %Area
B2O3 193.4000 1.6000 66.425 21.29
BC2O 190.1410 1.5000 8.825 2.83
Mg2B2O5 192.5641 1.5000 127.479 40.87
B-C SWNT 191.6074 1.6000 109.214 35.01
B 1s
CPS
Binding Energy (eV)

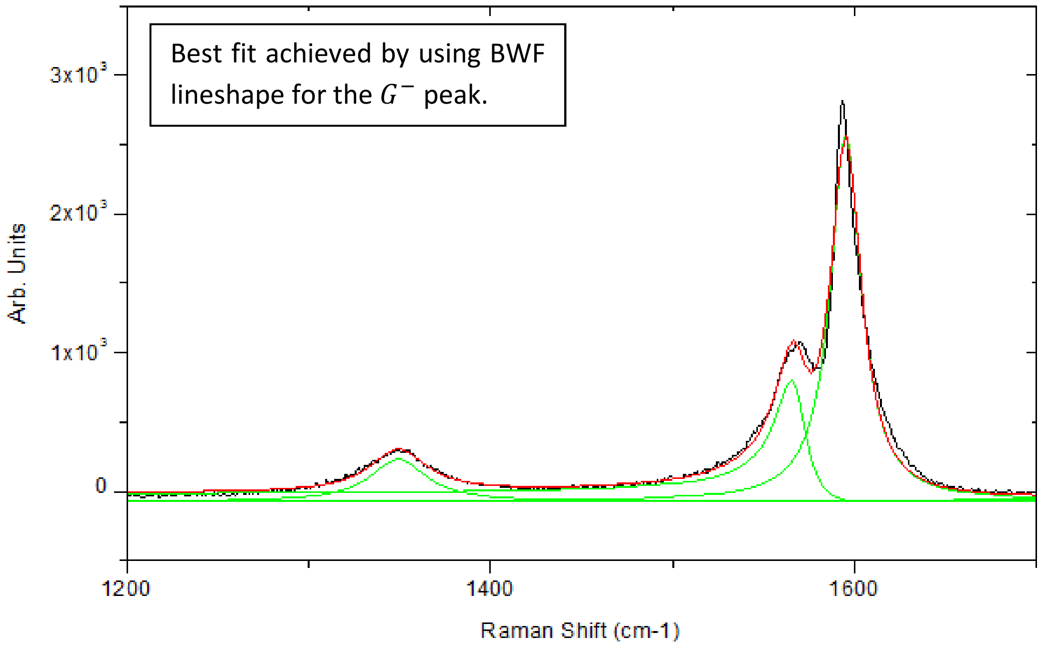
Best fit achieved by using BWF lineshape for the $G^-$ peak.
Arb. Units
3x10³
2x10³
1x10³
0
1200
1400
1600
Raman Shift (cm-1)

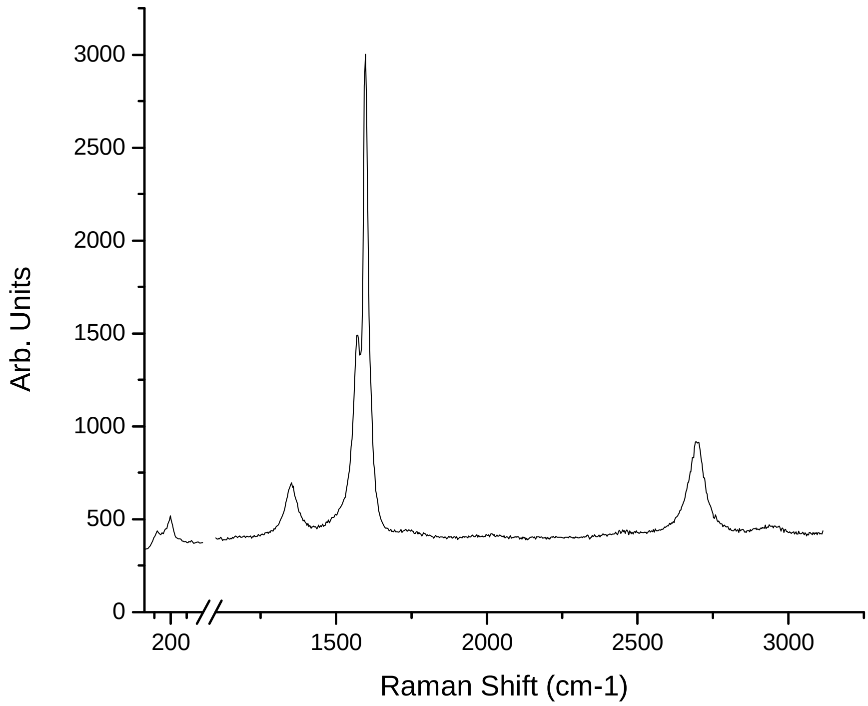
Arb. Units
3000
2500
2000
1500
1000
500
0
200
1500
2000
2500
3000
Raman Shift (cm-1)